


7-2015

# Capillary Electrophoresis for Analysis of A $\beta$ 1-42 Adsorption and Photo-Crosslinking

Jennifer Lynn Kurtz

*University of Arkansas, Fayetteville*

Follow this and additional works at: <http://scholarworks.uark.edu/etd>

 Part of the [Biological Engineering Commons](#), [Molecular, Cellular, and Tissue Engineering Commons](#), and the [Systems and Integrative Engineering Commons](#)

---

## Recommended Citation

Kurtz, Jennifer Lynn, "Capillary Electrophoresis for Analysis of A $\beta$ 1-42 Adsorption and Photo-Crosslinking" (2015). *Theses and Dissertations*. 1285.

<http://scholarworks.uark.edu/etd/1285>

This Thesis is brought to you for free and open access by ScholarWorks@UARK. It has been accepted for inclusion in Theses and Dissertations by an authorized administrator of ScholarWorks@UARK. For more information, please contact [scholar@uark.edu](mailto:scholar@uark.edu).

Capillary Electrophoresis for Analysis of A $\beta$ <sub>1-42</sub> Adsorption and Photo-Crosslinking

A thesis submitted in partial fulfillment  
Of the requirements for the degree of  
Master of Science in Biomedical Engineering

by

Jennifer Kurtz  
University of Arkansas  
Bachelor of Science in Chemical Engineering, 2012

July 2015  
University of Arkansas

This thesis is approved for recommendation to the Graduate Council.

---

Dr. Christa Hestekin  
Thesis Director

---

Dr. Jeffrey Wolchok  
Committee Member

---

Dr. Timothy Muldoon  
Committee Member

---

Dr. Shannon Servoss  
Committee Member

## Abstract

The accumulation of amyloid-beta ( $A\beta$ ) oligomers is believed to be the driving force behind Alzheimer's disease (AD) pathogenesis. Due to the metastable nature of  $A\beta$  oligomers, the knowledge of  $A\beta$  aggregation and accumulation is not well understood. Here, we use capillary electrophoresis (CE) and photo-induced crosslinking of unmodified proteins (PICUP) to learn about the aggregation of  $A\beta$ .

First, we explore the effect of capillary coating on  $A\beta_{1-42}$  protein loss using CE. The dynamic coatings tested were PHEA and 50 kDa, 2000 kDa, 5000 kDa, and 8000 kDa PEO. The covalent coating tested was PVA. The results indicated that 2000 kDa PEO allowed for the best recovery of  $A\beta_{1-42}$  with 87%. This was better than the uncoated capillary recovery of 66%, but less than the optimal 90%. The biggest issue encountered was a protein recovery of greater than 100%, which is theoretically impossible. More procedure development should be done to solve this problem.

Next, the PICUP reaction was optimized for analysis of  $A\beta_{1-42}$ . Using a novel approach, the goal was to apply PICUP to capture  $A\beta_{1-42}$  oligomers and correlate bands via SDS-PAGE analysis to peaks via CE analysis. The results showed that reactants needed for successful PICUP application interfered with CE detection of  $A\beta_{1-42}$ . We tested alternate reactants and several methods of removing reactants after PICUP application. We learned that dialysis was the most promising method of  $A\beta_{1-42}$  detection via CE after PICUP.

## Table of Contents

Chapter 1: Introduction.....	1
Alzheimer’s Disease .....	1
Capillary Electrophoresis.....	6
Photo-Induced Cross Linking of Unmodified Proteins .....	7
Purpose.....	8
Chapter 2: Polymer Capillary Coating Study.....	9
Introduction.....	9
Materials and Methods.....	14
Results and Discussion .....	17
Control .....	17
PHEA .....	22
PEO.....	23
50kDa.....	24
2000kDa.....	25
5000kDa.....	26
8000kDa.....	27
PVA .....	28
Chapter 3: Photo-Induced Cross Linking of Unmodified Proteins.....	31
Introduction.....	31
Materials and Methods.....	36
Results and Discussion .....	38
Future Directions .....	57
References.....	59
Appendix.....	62

## Chapter 1: Introduction

Alzheimer's disease (AD), a neurodegenerative disorder and most common form of dementia, is characterized by progressive memory loss, ultimately ending in death. (1) Approximately 500,000 people die each year from AD, making it the 6<sup>th</sup> leading cause of death in the United States. Additionally, AD is the only cause of death in the top ten that cannot be prevented, slowed, or cured. Between 2000 and 2010, Alzheimer's deaths increased by 68% while deaths from breast cancer, prostate cancer, heart disease, stroke, and HIV decreased. AD is already the most expensive condition in the nation costing \$214 billion in 2014 and is forecasted to cost \$1.2 trillion in 2050.

AD belongs to a larger class of diseases known as protein conformational disorders (PCDs). Other PCDs include Huntington disease, ALS, Parkinson disease and type II diabetes. PCDs are caused by a change in the secondary and/or tertiary structure of protein without change of the primary structure. Typically, PCDs cause a transformation from  $\alpha$ -helices to  $\beta$ -sheets. Misfolded proteins rich in  $\beta$ -sheets are termed amyloids, which are more specifically, tissue deposits of rigid protein fibrils 5-10 nm in diameter. (2) In the native  $\alpha$ -helix structure, the hydrogen bonds are between groups within the same strand. Hydrogen bonds in the  $\beta$ -sheets are between one strand and another. In most PCDs the misfolded protein becomes deposited in amyloid-like aggregates inducing tissue damage and organ dysfunction. (3)

AD is characterized by a few structural changes in the brain. First, neurons of the central nervous system begin to die causing alterations in synaptic inputs. Additionally, cell bodies and dendrites of these neurons contain neurofibrillary tangles (NFT) and the brain contains extracellular deposits of amyloid-beta ( $A\beta$ ). (4) The memory loss seen in patients with AD is due to neuronal loss in regions related to memory and cognition, neurotransmitter depletion, and

synaptic alteration. (5) The cause of this neuronal loss could be due to one or many of the structural abnormalities seen in AD brains post mortem. The presence of A $\beta$  plaques and intracellular NFT containing phosphorylated tau has been of most interest in the determining the causes of these changes. (6) The exact method in which A $\beta$ , NFT and/or phosphorylated tau cause neuronal death is unclear. (4) Cloning of the gene that codes for A $\beta$  and its location on chromosome 21, as well as the fact that Down Syndrome invariably leads to AD, led researchers to pursue the hypothesis that A $\beta$  accumulation is the key event in AD etiology. (7) This knowledge supports the amyloid hypothesis, which suggests that the accumulation of A $\beta$  in the brain is the driving force behind AD pathogenesis and formation of NFT is a result of the imbalance between A $\beta$  production and A $\beta$  clearance. The amyloid cascade hypothesis proposes the sequence of events resulting in AD is as follows: mutations in amyloid precursor protein (APP), presenilin (PS) 1, or PS2 genes, increased A $\beta_{1-42}$  production, A $\beta_{1-42}$  oligomerization and plaque formation, subtle effects of A $\beta_{1-42}$  oligomers on synapses, microglial and astrocytic activation, progressive synaptic and neuronal injury, altered neuronal homeostasis, altered kinase and phosphatase activity, widespread neuronal dysfunction and cell death, dementia. (7)

Specifically, A $\beta$  is a normal product of cleavage from APP. (5) A $\beta$  can be measured in cerebrospinal fluid, plasma, and culture medium. (7) APP is a naturally occurring 695-770 amino acid peptide that is encoded on chromosome 21. (5) The function of APP in the nervous system is unknown. Some studies have reported that APP has a role in signal transduction pathways and the growth of neuronal and non-neuronal cells. (4) Typically, APP predominately follows a non-amyloidogenic pathway where it is cleaved by  $\alpha$ -secretase, which does not result in the formation of A $\beta$ . (5) Conversely, when APP follows the amyloidogenic pathway, it is first cleaved by  $\beta$ -secretase creating a 99 amino acid peptide. The intermediate peptide is subsequently cleaved by

$\gamma$ -secretase creating  $A\beta$ . Depending on the point of cleavage by  $\gamma$ -secretase,  $A\beta$  monomer of 38, 40, or 42 amino acids is produced. (8) The 42 amino acid monomer is 4.5 kDa and has the following sequence:

DAEFRHDSGYEVHHQKLVFFAEDVGSNKGAIIGLMVGGVVIA

Figure 1: Amyloid-beta 1-42 amino acid sequence (6)

$A\beta_{1-40}$ , is the most abundantly produced isoform, but  $A\beta_{1-42}$  is more likely to oligomerize and form amyloid fibrils in the brain parenchyma. (8, 9) Additionally, mutations in PS proteins, specifically PS1 and PS2, have a direct effect on  $\gamma$ -secretase altering APP metabolism to produce amyloidogenic  $A\beta$ . (7) Even though  $A\beta$  production is a naturally occurring process, the overproduction of  $A\beta$  or increased proportion of  $A\beta_{1-42}$  has been shown to cause early onset AD. (7)

The amyloid hypothesis provides a framework for the cascade of  $A\beta$  causing AD, but the detailed process has yet to be discovered and agreed upon. The biggest criticism of the amyloid hypothesis is the amount of insoluble  $A\beta$  plaques found in the brain post-mortem does not correlate with the severity of symptoms the patient experiences during life. The amyloid hypothesis is also lacking in detail because a specific neurotoxic species of  $A\beta$  or its effect on neurons has not been clearly defined *in vivo*. (7) Research has supported the idea that a possible precursor, soluble  $A\beta$  oligomers, is the primary toxic species as it appears to correlate with cognitive impairment. To form fibrils and plaques,  $A\beta$  must accumulate, but the aggregation pathway  $A\beta$  monomer follows to form  $A\beta$  oligomer and  $A\beta$  fibril has been difficult to elucidate due to the metastable nature of the  $A\beta$  protein aggregates. Even though  $A\beta$  oligomers are kinetic intermediates for fibril formation, it has been suggested they are not necessary intermediates for

fibril formation. (10) Since oligomer formation is a dynamic process, it is likely that many different species exist simultaneously, making neurotoxicity difficult to pin on one form. (7) Additionally, all AD-causing mutations in APP, PS1, or PS2 increase A $\beta$  deposition, but there is no correlation with when AD symptoms begin to occur. (7) Neuronal death is present only in the advanced form of AD and is hypothesized to evolve only after decades of damage. It is suggested that A $\beta$  toxicity is subtle until damage associated with oligomer stress and accumulation occurs which causes the irreversibility of neurodegeneration. (6) Overall, there are large gaps in the amyloid hypothesis for understanding the pathogenesis of AD. However, none of the criticisms of the amyloid hypothesis are large enough to discount the theory and simply relay the lack of understanding surrounding AD.

Indeed, even though the amount of insoluble A $\beta$  does not correlate with AD symptoms, many studies have supported that a soluble oligomer is the toxic species. (11) Research suggests memory impairment occurs early and is attributed to nerve cell death. (9) Synthetic A $\beta$ , termed AD diffusible ligands (ADDLs), intermediates and fibrils cause minor injury to cultured neurons. (7) Soluble, A $\beta$  oligomers are shown to inhibit synaptic function by consistent aberrant signaling leading to early memory deficits and synaptic degradation. (12) Campioni et al. determined that when oligomers are produced intracellularly, flexible hydrophobic surfaces of A $\beta$  are exposed that might contribute to trapping vital proteins. When A $\beta$  oligomers are produced extracellularly, they cause toxic alterations of cell membranes. (13) Likewise, transgenic mice studies have shown memory impairment and changes in neuron form before fibrillar A $\beta$  is deposited. (8) *In vivo* rat studies indicate that human A $\beta$  oligomers can inhibit long-term potentiation in the hippocampus, which is necessary for memory formation. This determination



was made without the presence of A $\beta$  monomers or fibrils, confirming that oligomers are the toxic A $\beta$  species. (7)

Extractions of AD brain tissue contain a large amount of soluble A $\beta$  between 10-100 kDa, the majority of which existed in the dodecameric form. (12) In studies on AD brains, the soluble A $\beta$  level in the frontal cortex was increased three fold compared to non-AD controls and there was no correlation in the amount of soluble and insoluble A $\beta$ . (14) In contrast, Kasai et al. reported lower levels of soluble A $\beta$  in cerebrospinal fluid of AD patients. (15) The decrease of A $\beta$  in CSF is thought to be due to the deposition of A $\beta$  in plaques and limiting its ability to diffuse into CSF. (16) Walsh et al. showed that nonamer and decamer levels correlated with spatial memory impairment when compared to monomer, trimer, and hexamer. However, nonamer and decamers were not shown to correlate with other types of memory loss or synaptic function loss. (8) It is possible that smaller order oligomers are the cause of other types of memory impairment. Neurons in the medial temporal lobe and hippocampus are particularly susceptible to loss in AD and their loss seems to coincide with cognitive impairment. (16) Overall, experiments support the existence of soluble A $\beta$  oligomers, but their direct effect on neuronal toxicity has yet to be determined. (6)

The A $\beta$  aggregation pathway to form these toxic oligomers and insoluble fragments found in AD brains is largely unclear. The starting point is a native and active conformation consisting of  $\alpha$ -helical and random structure and the ending point is the same protein in a pleated  $\beta$ -sheet conformation, typical of PCDs. (3) There are two known regions of A $\beta$  that play a role in aggregation and formation of fibrils. The C-terminal end plays a role in the rate of aggregation. Therefore, A $\beta$ <sub>1-42</sub> aggregates much faster than A $\beta$ <sub>1-40</sub>, as mentioned earlier. Additionally, hydrophobic residues 16-23 are essential in peptide misfolding and the polymerization of A $\beta$ . (5)

Studies in human, transgenic mice, and cell culture show that soluble and insoluble A $\beta$  exist in equilibrium. (14)

It should be noted that terminology of A $\beta$  structures is widely varied in published studies. Here, oligomers refer to the structure between monomer form and insoluble fibril form. It should also be noted that slight changes in A $\beta$  concentration and preparation can lead to differences in resulting A $\beta$  distribution and therefore experimental results. There is no method that prepares oligomeric A $\beta$  in a physiological condition because the low nanomolar levels in the brain are much lower than the micromolar levels needed for *in vitro* studies. (12) The low concentration of A $\beta$  oligomers and potent neurotoxicity make them a viable therapeutic target. It is vital to understand this pathway in order to understand AD etiology and design a potential drug to block the toxic effects of A $\beta$ .

### **Capillary Electrophoresis**

Capillary electrophoresis (CE) is an efficient and inexpensive way to separate protein species based on their size and charge. CE creates a voltage between two buffer vials, which induces a current to pull the protein through a capillary. The smaller, higher charged species elute first and the larger, lower charged species elute last. The species are detected, in this case, via UV absorption at 214 nm. CE cannot give specific information about the molecular weight of the species, only the proteins relative size to charge ratio to other species in the sample.

Previous studies have shown CE is capable of monitoring A $\beta$  aggregation. (17) However, CE requires a micromolar concentration of A $\beta$  rather than the physiological low nanomolar to picomolar concentrations. Additionally, A $\beta$  is a hydrophobic protein and can stick to the negatively charged walls of the capillary rendering a false representation of the sample injected.

Coating the capillary with a hydrophilic polymer will reduce the loss of A $\beta$ , increase the ability to see more of the aggregated species, and reduce the potential for A $\beta$  to become unattached from the capillary wall and ruin subsequent capillary runs. Ultimately, reducing the loss is essential for A $\beta$  detection at a physiological concentration

Polyethylene oxide (PEO) and poly-N-hydroxyethylacrylamide (PHEA) are dynamic coating polymers that form an adsorptive layer on the capillary and show minimal protein adsorption as well as suppression of electroosmotic flow (EOF). (18) Polyvinyl alcohol (PVA) is a covalent coating that becomes chemically bonded to the capillary wall after a heat treatment and has also been shown to decrease protein adsorption. (19) Determining an appropriate capillary coating for CE that increases the amount of protein recovered will allow for a physiological sample of A $\beta$  to be studied. This coating can be translated to the development of a microchip electrophoresis (ME) system that has the ability to detect metastable A $\beta$  species at a physiological, nanomolar scale. Ultimately, the ME system could lead to a commercially available system to enhance AD studies worldwide.

### **Photo-Induced Cross Linking of Unmodified Proteins (PICUP)**

Due to the metastable nature of A $\beta$ , aggregation states have been difficult to elucidate, as discussed previously. Photo-Induced Cross Linking of Unmodified Proteins (PICUP) is a method with promising ability to stabilize A $\beta$  at a specific time point and allow the aggregation pathway to be studied. (20) PICUP utilizes photoexcitation of a ruthenium compound in the presence of an electron acceptor creating a virtual snapshot of the protein structure at the time A $\beta$  is exposed to a brief flash of light. Ultimately, PICUP has the ability to cross-link A $\beta$  in its native state (that

is without the addition of chemical crosslinking agents). PICUP provides the crucial ability to study A $\beta$  in a fixed conformation, non-metastable state along the aggregation pathway.

Typically, after PICUP is performed on A $\beta$ , the samples are run on an SDS-gel and the molecular weights of A $\beta$  at different aggregation time points are determined. However, the SDS-gel denatures the protein and removes the secondary and tertiary structure. If PICUP samples were analyzed via CE, the secondary and tertiary structure would remain intact. Correlating a SDS-gel with CE could give more information about the specific sizes of species present, their charges, and their amounts.

## **Purpose**

Chapter 2 summarizes a study performed using CE that tested the coating abilities of different hydrophilic polymers in order to minimize A $\beta$  loss in capillaries. Capillaries were dynamically coated with PHEA and PEO, which previously have shown the ability to lower A $\beta$  adsorption. Polyvinyl alcohol was also studied as a covalent coating. In this study, a protein recovery of 90% was considered desirable. Minimal loss of A $\beta$  is essential to be able to detect A $\beta$  at a physiological concentration and ultimately develop a microchip electrophoresis system for commercial use.

Chapter 3 summarizes the use of PICUP to capture A $\beta_{1-42}$  transient species on an SDS-gel. It also discusses the novel ability to detect PICUP samples using CE and compare the results with traditional SDS gels. CE could provide a higher resolution and non-denaturing analysis of A $\beta_{1-42}$  species. Correlating SDS-gel and CE will give insight into size of the species present and development of a model to predict the molecular weight of A $\beta_{1-42}$  species along the aggregation pathway.

## Chapter 2: Minimizing Protein Loss

### Introduction

Capillary electrophoresis (CE) is an efficient way to separate protein species based on their size and charge, known collectively as electrophoretic mobility. Polyacrylamide gel electrophoresis (PAGE) has been the predominate technique to separate protein species based on their size. However, CE has many advantages over PAGE such as: shorter analysis times, easier automation, and lower usage of chemicals. Additionally, CE allows for analysis of proteins in their native state where the SDS in PAGE analysis denatures the protein and can remove the secondary, tertiary, and quaternary structure.

Capillary electrophoresis begins by injecting a protein sample into a capillary. The capillary is then filled with buffer and both ends are placed into buffer vials. A voltage is applied between the buffer vials and current is induced to initiate protein migration from the anode to the cathode, meaning positive ions elute first followed by neutral species then anions. The protein species separate and are detected by UV absorption at 214 nm using a Deuterium lamp. The output of the detector is an electropherogram showing protein absorbance as a function of time.

The electrophoretic mobility ( $\mu$ ) of the protein species can be approximated by the Debye-Huckel-Henry theory:

$$\mu = \frac{q}{6 \pi \eta r} \quad (1)$$

where  $q$  is the charge of the species,  $\eta$  is the viscosity of the buffer, and  $r$  is the Stokes' radius of the species. (21) A closer look at this equation shows a highly charged, small particle will have a high mobility and elute first and a lower charged, large particle will elute last. Considering all ions pass the detector, there must be a force sweeping anions towards the cathode since they

should naturally repel. This force is called electroosmotic flow (EOF) and propels all ions regardless of charge towards the cathode.

The EOF is caused by interactions between the buffer and the glass wall of the capillary and results in low separation efficiency, which is the largest disadvantage to CE analysis. Low resolution of the separation can also be caused by hydrophobic and electrostatic interactions between the protein and wall of the capillary. (22) In more detail, fused silica capillaries have a negative charge due to the ionization of silanol groups when in solution. When the capillary is filled with buffer, the cations of the buffer are drawn towards the silanol groups and form a double layer of cations. When a voltage is applied between the anode and the cathode, the first layer is held tightly by electrostatic interactions and the second layer is drawn towards the cathode. The flow of the second layer of cations is referred to as the EOF and causes the bulk flow of ions towards the cathode. Assuming the EOF is larger than the electrophoretic mobility of the protein, all protein species will be drawn towards the detector. When the value of the EOF greatly dominates the protein's electrophoretic mobility, a high protein resolution is difficult to achieve. (23) Manipulation of the EOF is crucial to a fast and efficient protein separation.

Due to the negative charge of the capillary's silanol groups and the positively charged layer supplied by the buffer, protein species can adsorb to the walls of the capillary resulting in protein loss. Typically, protein adsorbs to the capillary via electrostatic interaction, but hydrogen bonding and hydrophobic interactions with already adsorbed protein can also occur. (24)

In order to overcome low separation efficiency, protein adsorption is slowed and the EOF is suppressed by modifying the inside surface of the fused silica capillary. An attractive way to modify the capillary surface is to add polymeric coatings that compete with the protein for interaction with the silanol groups on the capillary wall. The availability of the protein to adsorb

to the capillary wall is minimized because it now has a neutral charge. The EOF is suppressed by the polymer coating increasing the solution viscosity in the first layer of ions without affecting the viscosity of the second layer. It is essential that a highly acidic treatment is performed prior to polymeric treatment to increase the silanol group availability for hydrogen bonding with the polymer. (22)

The suppression of EOF and minimization of protein loss is essential to detect protein present in low concentrations, such as the physiological nanomolar range of  $A\beta_{1-42}$ . The suppression of EOF can be measured by comparing the electrophoretic mobility of a protein in a coated versus uncoated capillary. The adsorption of protein to capillary walls is measured by comparing the area under peaks of the electropherogram after injecting the protein at the inlet and outlet of the capillary. When the protein is injected at the inlet of the capillary, the protein travels 21 cm from the anode to the detector. When the protein is injected at the outlet of the capillary, the voltage is reversed and the protein travels 10 cm from the anode to the detector. (See Figure 2 as a reference.)

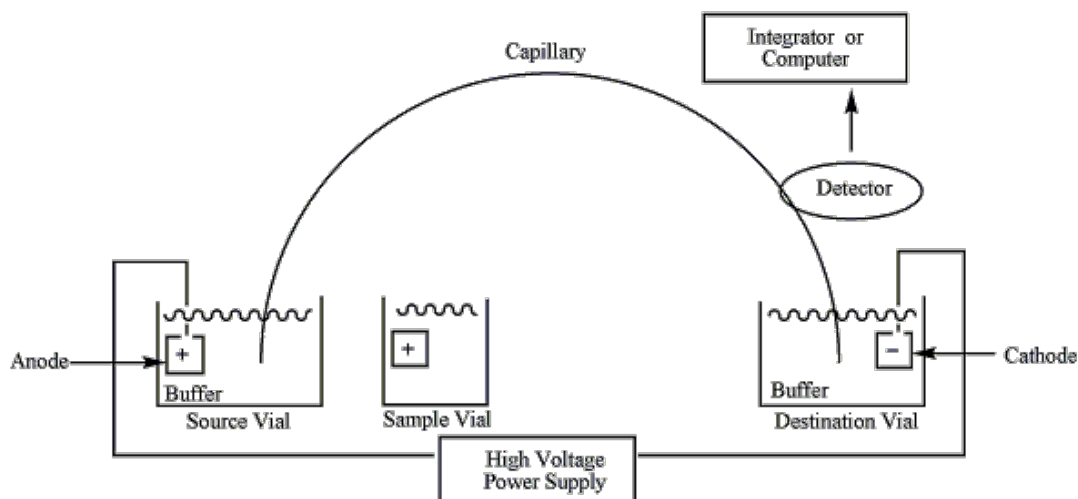


Figure 2: This is a schematic of capillary electrophoresis. When the sample is injected on the long side, it travels from the source vial to the destination vial. When the sample is injected on the short side, the cathode and anode are switched. Then, the sample is injected in the destination vial and travels to the source vial. (25)

The differences in the length of capillary allows for different amounts of protein to be adsorbed onto the capillary wall. Bohoyo et al. provide equation 2 to calculate the recovery percentage of the protein.

$$X = 100 * (A_L/A_S)^2 \quad (2)$$

where  $A_L$  and  $A_S$  are the peak area in the long and short capillary lengths, respectively. (26) A protein recovery of 90% is considered desirable in this study. This assumes a representative sample is injected on both the long and short runs.

Two approaches to surface modifications are dynamic and covalent hydrophilic polymer coatings. Dynamic capillary coatings suppress the negative charge of the capillary wall by electrostatic interactions with the capillary's negatively charged silanol groups and covalent coatings permanently suppress the negative charge by covalently bonding to the fused silica. Typically, dynamic coatings are preferred to covalent coatings due to their simplicity and speed of the protocol. However, covalent coatings are permanent and better suited for long studies. It is important to optimize the adsorption properties of the polymer and the thickness of the coating layer to achieve proper protein separation. The hydrophilic-hydrophobic balance of the polymer, the polymer's potential for hydrogen bonding with the capillary wall, and the nature of the solvent should also be considered when choosing a polymeric coating. An ideal coating would balance the ease of a dynamic coating with the longevity of a covalent coating. (22)



EOF suppression and protein recovery calculations were performed to evaluate the effectiveness of each coating. The dynamic hydrophilic polymers used in this study were poly-n-hydroxyethylacrylamide (PHEA) and polyethylene oxide (PEO), both uncharged coatings. PHEA has a high hydrophilicity and has been shown to be favorable for suppression of protein adsorption. (27)

PEO can form a dynamic coating due to its ability to hydrogen bond with the silanol groups along the capillary wall. A dynamic PEO coating has been shown to be more effective than a covalent PEO coating at suppressing the EOF. (27) Therefore, only a dynamic PEO coating was used in this study.

The covalent coating tested in this study is polyvinyl alcohol (PVA), as it is considered to be the most hydrophilic polymer. (28) Steiner et al. showed PVA was the most efficient in EOF control in aqueous systems when compared to vinyl, vinyl acetate, and acrylates. (23) A covalently coated PVA capillary has been shown to have superior separation of basic proteins over a wide pH range and last for over 1000 runs. (28) The capillary must be acidified with glutaraldehyde as a cross-linking agent prior to PVA treatment. The coating occurs at the interface between the glutaraldehyde and PVA solutions, creating a uniform layer along the capillary wall. (27) It is necessary to treat the capillary with heat up to 160°C so the poly vinyl alcohol becomes water insoluble. At temperatures higher than 160°C, the polymer starts to degrade. (19) Since PVA coating procedure is performed by hand versus by the CE machine, it is prone to human error. Additionally, PVA is first adsorbed onto the capillary wall before thermal treatment, the coating procedure itself is prone to inconsistencies. (27) The potential for inconsistent coating errors should be taken into account when performing the procedure and analysis.

Determining the best polymeric capillary coating is essential to reducing the loss of protein via capillary wall attachment and therefore accurately detecting A $\beta$ <sub>1-42</sub> aggregates. The purpose of this study is to determine a coating that effectively reduces EOF and provides at high recovery of A $\beta$ <sub>1-42</sub>. Ultimately, this knowledge will be applied to the development of a microchip electrophoresis system, which has the ability to detect A $\beta$ <sub>1-42</sub> in its physiological nanomolar concentration.

## **Materials and Methods**

### *Amyloid beta preparation*

Amyloid beta (Anaspec, Fremont CA, Lot #1360300 and 1472260), was stored at -80°C. To ensure samples were monomeric a 1 mg/mL stock of amyloid beta was prepared in Hexafluoro-2-propanol (HFIP). Amyloid beta was aliquotted into vials containing 0.0271 mg and the HFIP was allowed to evaporate in the hood overnight. The amyloid beta was brought up to a concentration of 20  $\mu$ M with 10 mM phosphate buffer.

### *Capillary Electrophoresis*

Capillary electrophoresis was performed using a Beckman P/ACE MDQ (214 nm filter). The machine was interfaced with an IBM computer and Beckman Coulter 32.0 Karat software (Version 5.0). Samples were pressure injected for 35 seconds at 0.5 psi. Long runs were separated at 7 kV for 60 minutes and short runs were separated at 7 kV for 30 minutes in a 31 cm fused silica capillary of 50  $\mu$ m diameter. Long and short runs were alternated with a capillary rinse in between to wash out any residual protein not detected. The capillary rinse consisted of deionized water wash for 10 minutes at 50 psi then 100 mM phosphate buffer wash for 10

minutes at 50 psi. Long and short runs were examined in triplicate resulting in six runs per capillary. Each coating was tested on two capillaries.

The dynamic coating process was initiated by a preconditioning rinse in the CE machine. The preconditioning rinse consisted of: 20 minutes at 50 psi with 0.1M NaOH, 20 minutes at 20 psi with deionized water, and 60 minutes at 20 psi with 0.1M HCl. The coating step started with a 15 minute deionized water wash at 20 psi, then a 15 minute 0.1M HCl rinse at 20 psi. The capillary was then rinsed with the coating of choice for 30 minutes at 50 psi. Next the capillary was rinsed for 15 minutes at 20 psi with deionized water. The capillary then was rinsed for 10 minutes with deionized water followed by a 10 minute polymer rinse.

The covalent coating process was developed in house based on work by Belder et al. (28) A custom built device to coat the capillary was influenced by one described by Buchholz et al. (29) A nitrogen gas port was attached on the outside of the device leading into a chamber filled with polymer solution, as seen in Figure 3. The capillary was inserted into the chamber and sealed airtight. When nitrogen was applied to the system, the solution was forced through the capillary. The 0.5% PVA procedure slightly modified from Belder is as following: push aqueous glutaraldehyde solution through capillary with 100 psi of N<sub>2</sub> for 30 minutes, purge the capillary with N<sub>2</sub> at 100 psi for 10 minutes, push an acidified PVA solution through the capillary with 100 psi of N<sub>2</sub> for 30 minutes, purge the capillary with N<sub>2</sub> at 100 psi for 10 minutes. Afterwards, the capillary was put in an oven and heated from 25°C to 160°C for over 20 minutes.

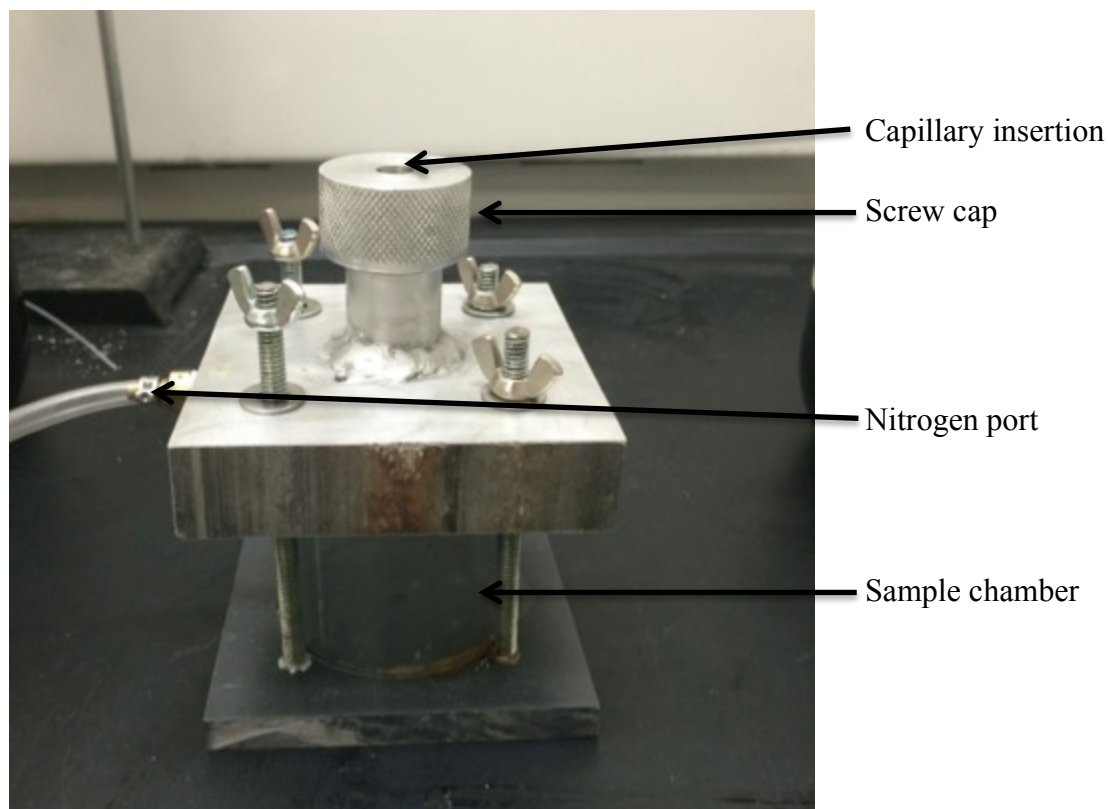


Figure 3: The device created in house to coat capillaries with .5% PVA is shown above. The nitrogen attachment is located on the left. The capillary is inserted through a rubber stopper at the top into the bottom chamber containing the coating solution. The attachment at the top can then be turned to create an airtight seal. The entire device is turned horizontally when coating so gravity is not acting against the direction of flow.

#### *Data Analysis*

Capillary electrophoresis data was analyzed using Origin 9.0 and Microsoft Excel. The data was imported into Origin, where the noise baseline was subtracted from the data set to produce a constant baseline of zero. This data was copied into excel where it was plotted versus time. In Origin, the peak was fitted to a bigaussian curve because this curve had the best fit to the peaks. The peak elution time, height, and area under the curve were recorded as well as the

noise of the data. The area was compared between long and short runs to calculate the recovery using equation 2. All long runs were plotted with a non-zero baseline to make the comparable peaks easier to visualize. The signal to noise ratio was calculated by taking the average of the signal from the start of the peak to the end of the peak and dividing it by the average of the baseline signal.

## **Results and Discussion**

The effect of capillary coating on protein adsorption was investigated. Peak height had to be at least three times the noise of the data to be considered acceptable signal. For short runs, the protein traveled 10 cm to the detector, and protein separation occurred for 30 minutes. For long runs, the protein traveled 21 cm to the detector, and protein separation occurred for 60 minutes. Most of the electropherograms were adjusted so only the first 15 minutes of data are shown.

### *Control*

The control condition was an uncoated capillary and therefore no suppression of the EOF. Figure 4 shows a representative electropherogram for a long and short run of unaggregated A $\beta$ <sub>1</sub>.

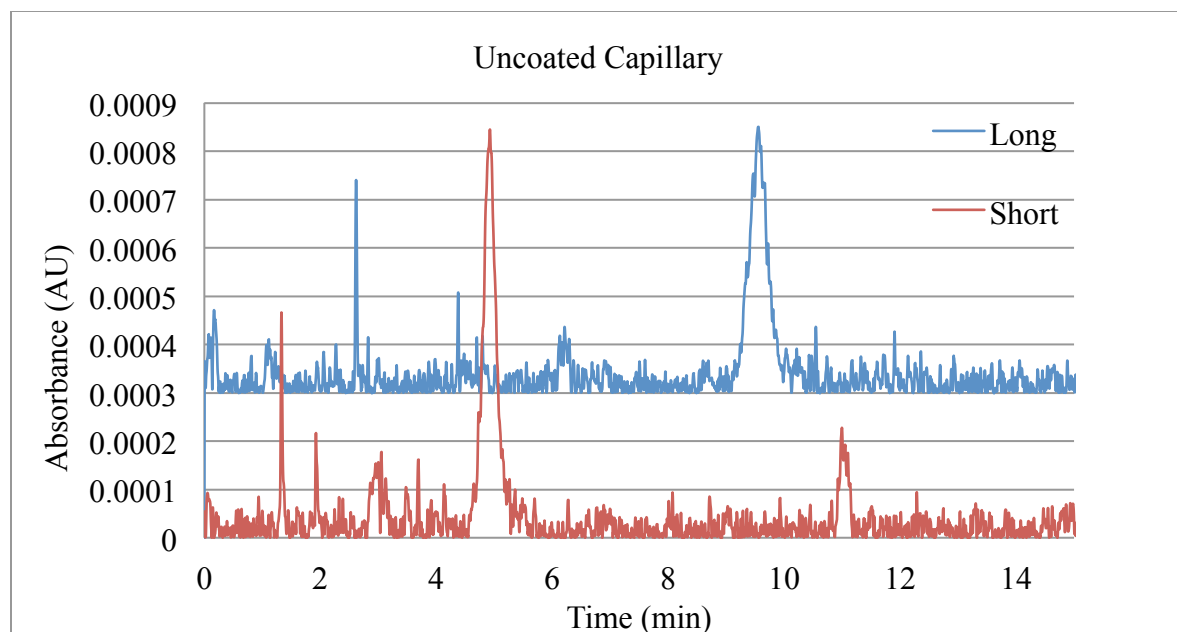


Figure 4: A representative electropherogram of  $A\beta_{1-42}$  on an uncoated capillary for lot #1360300 and an 8 second injection time. The short run analyzed the peak eluted around 5 minutes. The long run analyzed the peak eluted around 9 minutes.

Theoretically, the peak being examined is a monomer peak, however, due to the metastable nature of  $A\beta_{1-42}$ , the exact size of the species is unknown. Lot #1360300 was tested first. The peaks being compared are detected around 5 minutes and 9 minutes for the short and long runs, respectively, as shown in Figure 4. The average recovery of these peaks was 67.5% with a standard deviation of 4.98% ( $n = 3$ ). The significant discrepancy between observed peak recovery and ideal peak recovery show the importance of controlling the EOF and minimizing protein loss. In order confirm the results, an additional distinct capillary needed to be tested, but a different lot of  $A\beta_{1-42}$  had to be used. Figures 5,6, 7, and 8 show  $A\beta_{1-42}$  from lot #1472260. This lot displayed vastly different results from lot #1360300. First,  $A\beta_{1-42}$  was not detected at the same concentration, 20  $\mu\text{M}$ , for an 8 second injection time. After copious amounts of testing to

be able to detect  $A\beta_{1-42}$ , the concentration was increased to  $40\ \mu\text{M}$  and injection time was increased to 35 seconds. Secondly, the two peaks compared were about 1.7 minutes and 3.5 minutes for the short and long runs, respectively. This peak elution is much shorter than the previous lot of  $A\beta_{1-42}$ . Similarly, long and short runs were alternated for a total of six runs. The first two runs had an  $A\beta_{1-42}$  recovery of 66%. However, when the next long and short runs were analyzed and compared, it was found that the recovery was greater than 100%. Theoretically, this is not possible which indicates an error in the experiment.

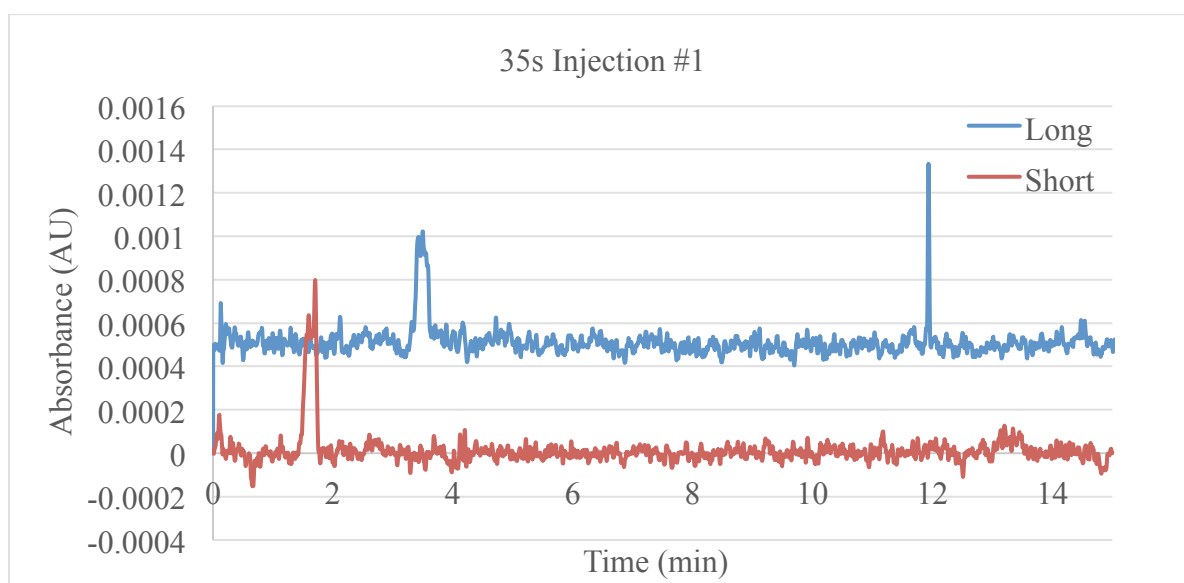


Figure 5: The first long run and short run electropherogram for an uncoated capillary where  $A\beta_{1-42}$  was injected for 35 seconds. The short run analyzed the peak eluted around 1.7 minutes. The long run analyzed the peak eluted around 3.5 minutes.

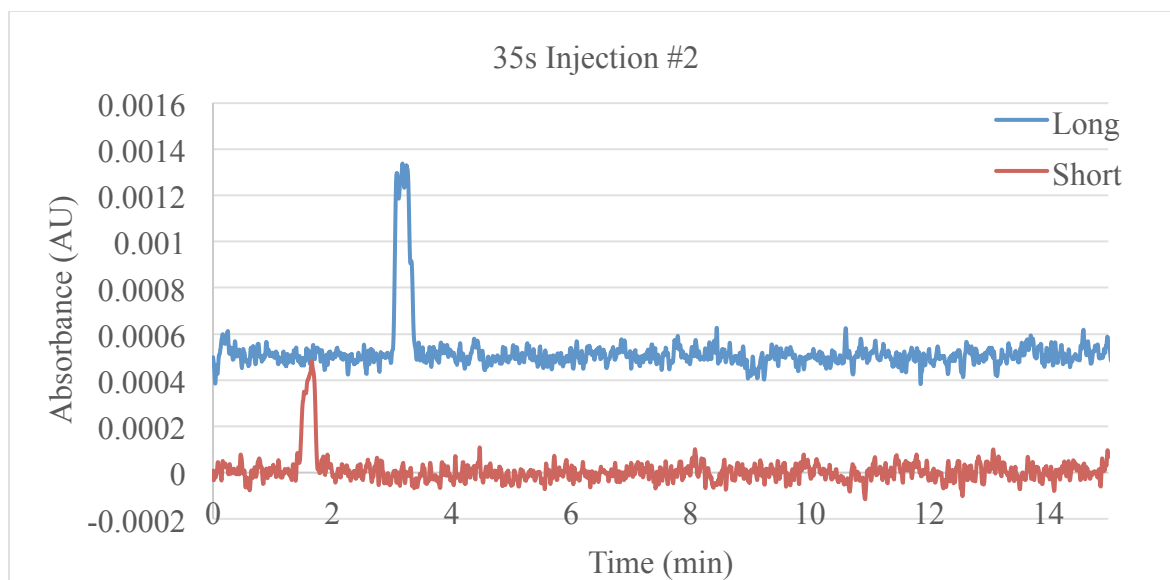


Figure 6: The second long run and short run electropherogram for an uncoated capillary where  $A\beta_{1-42}$  was injected for 35 seconds. The short run analyzed the peak eluted around 1.7 minutes. The long run analyzed the peak eluted around 3.5 minutes.

Table 1: The area and recoveries for the first two sets of uncoated capillary runs (Figures 4 and 5) where  $A\beta_{1-42}$  was injected for 35 seconds.

	Time	Area	Fit	Recovery
Short #1	1.70	1.38E-04	0.792	66.0
Long #1	3.45	1.12E-04	0.442	
Short #2	1.67	1.03E-04	0.714	489
Long #2	3.15	2.29E-04	0.779	

The first recovery of 66% for an uncoated capillary was expected. However, the second recovery of over 100% was not. As you can see the area for long run #2 is about twice as much as the area for long run #1. The peaks were fit to a bigaussian curve and since the noise for uncoated capillary data was large, the fit was not ideal. However, long #1 had a particularly bad fit. Additionally, the peaks were not as sharp as expected and had a somewhat flat top. In order to increase the fit, the injection time of  $A\beta_{1-42}$  was decreased to 25 seconds. These results are



displayed in Figures 7 and 8 and Table 2.

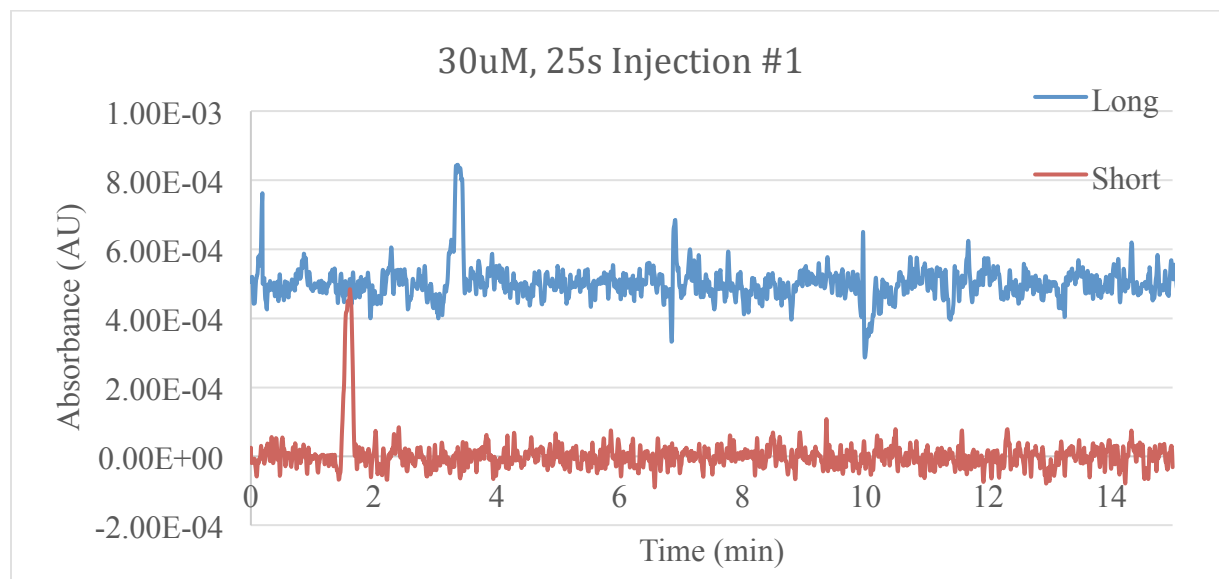


Figure 7: The first long run and short run electropherogram for an uncoated capillary where  $A\beta_{1-42}$  (lot #1462260) was injected for 25 seconds. The short run analyzed the peak eluted around 1.7 minutes. The long run analyzed the peak eluted around 3.5 minutes.

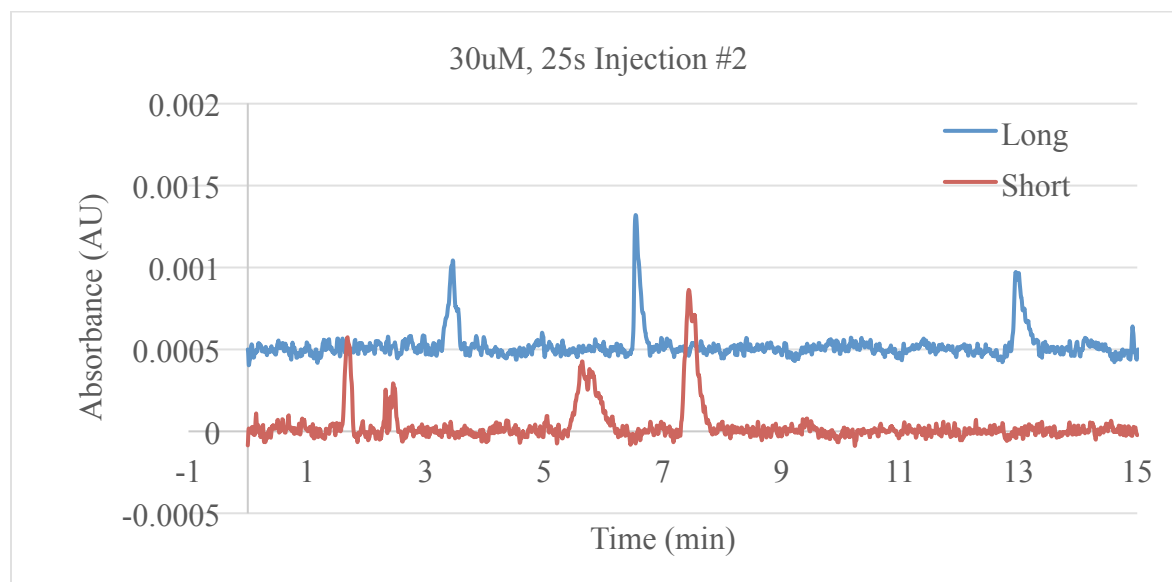


Figure 8: The second long run and short run electropherogram for an uncoated capillary where  $A\beta_{1-42}$  (lot #1462260) was injected for 25 seconds. The short run analyzed the peak eluted around 1.7 minutes. The long run analyzed the peak eluted around 3.5 minutes.

Table 2: The area and recoveries for the first two sets of uncoated capillary runs (Figures 6 and 7) where  $A\beta_{1-42}$  was injected for 25 seconds.

	Time	Area	Fit	Recovery
Short #1	1.61	6.87E-05	0.700	69.2
Long #1	3.39	5.71E-05	0.251	
Short #2	1.70	6.84E-05	0.943	150
Long #2	3.42	8.39E-05	0.640	

Interestingly, even though the peaks are more bell shaped and therefore more apt to fit a bigaussian curve, the data did not reflect it. The fit was still low. This suggests that the large noise present in the data is at fault for the insufficient fit of the peaks. It is also interesting that the second set of short and long runs had a recovery greater than 100%, similar to the runs where  $A\beta_{1-42}$  was injected for 35 seconds. It is possible that  $A\beta_{1-42}$  from a previous run is eluting during a later run and therefore creating a falsely high recovery. Additional experiments were performed lengthening the run time up to 60 minutes, but the results were the same. (Data not shown). More experiments should be performed to lengthen the rinse time between runs to see if this affects the recovery of  $A\beta_{1-42}$ .

### *12500 kDa PHEA*

Only lot #1360300 was tested with 12500 kDa PHEA as a coating. Figure 9 shows representative runs when a capillary is coated with 12500 kDa PHEA. The  $A\beta_{1-42}$  peak time elution and area were inconsistent when the capillary was coated with PHEA. The two peaks compared are the short peak around 5 minutes and the long peak around 10 minutes. The average recovery was 297% with a standard deviation of 262%. All runs except 1 resulted in protein recovery greater than 100%, which is impossible. There were 3 groups of long and short

runs able to provide a recovery. While more testing was done, some runs did not detect any  $A\beta_{1-42}$  providing no peaks for comparison or analysis. This polymer has a very high molecular weight which makes it more viscous than lower molecular weight polymers. Therefore it is likely that the polymer was not able to completely coat the capillary. Additionally, PHEA itself absorbs UV light at 214 nm which could lead to unrealistic recovery values or inconsistent results. Therefore, PHEA is not an acceptable polymeric coating for the purposes here.

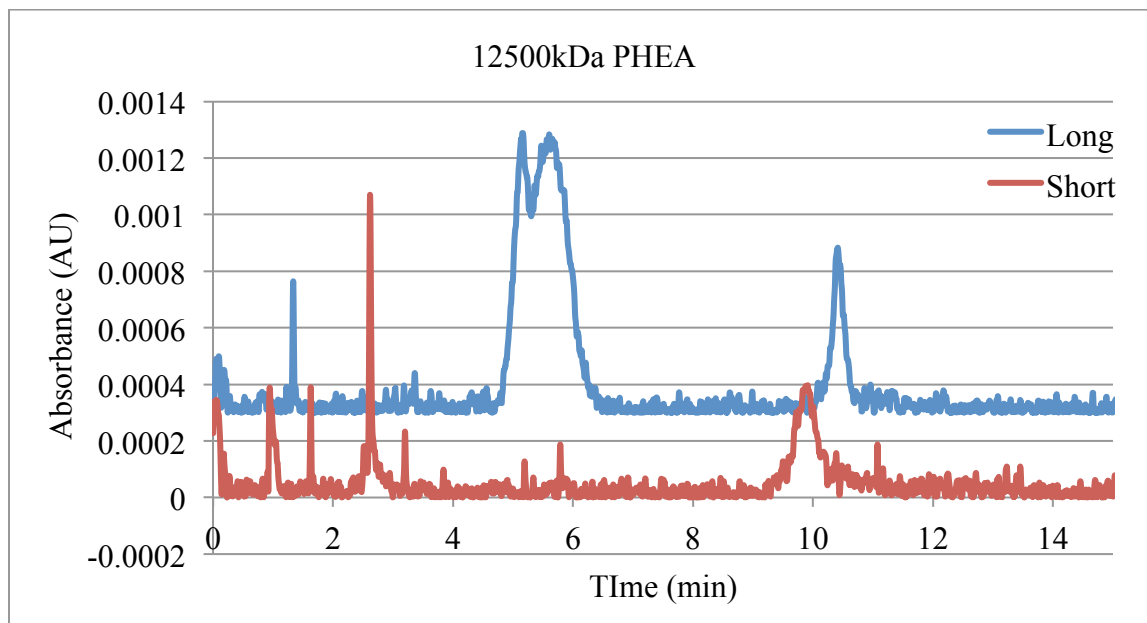


Figure 9: Representative electropherogram for a capillary coated with 12500 kDa PEO for lot #1360300 of  $A\beta_{1-42}$ . The peaks analyzed occurred at 5 minutes and 10 minutes for the short and long runs, respectively.

### *PEO*

Multiple molecular weights of PEO were available to test for capillary coating. Generally, the higher molecular weights served as better coating polymers due to their higher viscosity. However, if the viscosity was too high, an uneven coating was accomplished resulting in poor recovery of  $A\beta_{1-42}$ . Additionally, since  $A\beta_{1-42}$  is a small protein, a small molecular weight

PEO was tested to study the range of PEO. Only lot #1360300 of protein was tested for PEO coated capillaries since lot #1462260 was not providing adequate results on the simpler uncoated capillary.

### 50 kDa PEO

The smallest molecular weight of PEO tested was 50 kDa. The elution of peaks was inconsistent, making the ability to calculate recovery impossible. Only one set of runs eluted a peak on both the long and short version, these runs are shown in Figure 10. This set had a protein recovery of 46%. Only one long run had a peak detected, suggesting that all of the protein adsorbed to the walls of the capillary. The short runs had a large variation of peak elution time with the average being 13.1 minutes  $\pm$  2.17 minutes. The inconsistent detection of peaks is not desirable for a polymeric coating. Since only one set of runs was capable of analysis, 50 kDa PEO is not suggested as a polymeric coating.

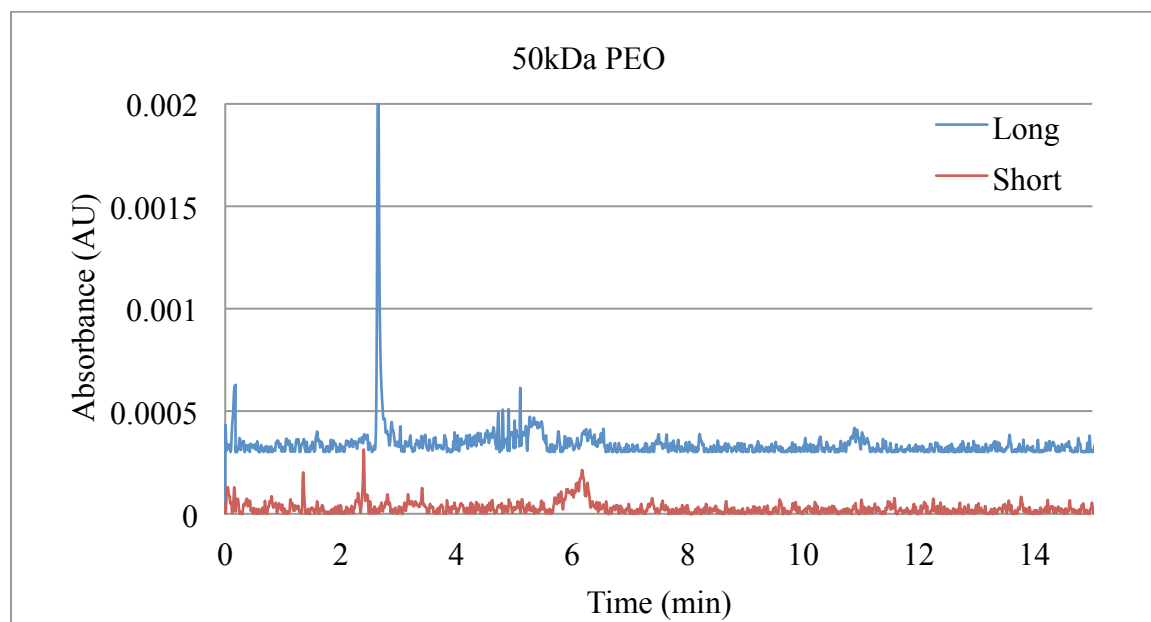


Figure 10: A representative long run and short run electropherogram for a capillary coated with 50 kDa PEO. Only one long run showed a peak, which eluted around 4 minutes. The short run

had a large variation of peak elution time.

### 2000 kDa PEO

The next molecular weight tested was 2000 kDa PEO. It was the best dynamic coating with a peak recovery of 87.4% and a standard deviation of 4.8%. The two peaks compared were the short run around 5 minutes and the long run around 10 minutes. Figure 11 shows the representative electropherograms for a capillary coated with 2000 kDa PEO. The peaks compared occurred at 5 minutes and 10 minutes for the short and long runs, respectively. Even though the average peak recovery is slightly less than the 90% ideal recovery, 2000 kDa PEO still showed the most promise as a coating. Out of this study, 2000 kDa PEO had the best protein recovery and performed better than an uncoated capillary. However, only three short and long run comparisons were able to be performed. Lot #1360300 of A $\beta$ <sub>1-42</sub> was not available for more experiments and lot #1462260 was showing vastly different results as shown in the uncoated capillary section.

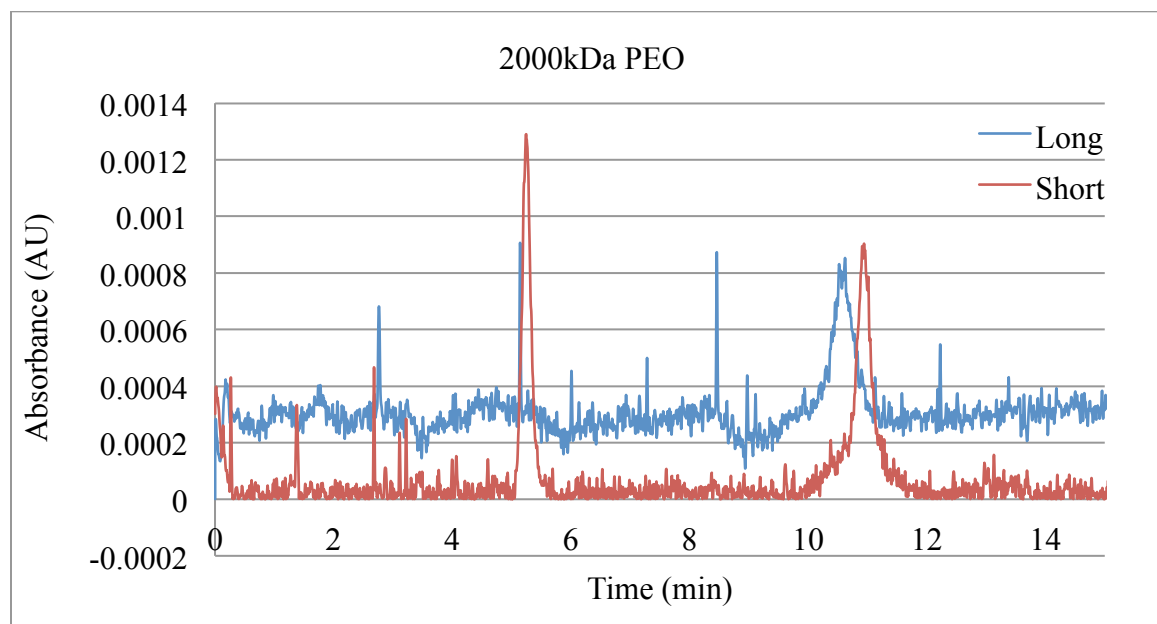


Figure 11: A representative long and short run electropherogram for a capillary coated with 2000

kDa PEO. The peaks compared occurred around 5 minutes and 10 minutes for the short and long runs, respectively.

### 5000 kDa PEO

Previously, the noise background was subtracted from the data for a constant baseline of zero. This was not performed with 5000 kDa PEO coated capillaries due to a peak abnormality. The peak abnormality made the peak area calculation user dependent because the peak beginning and end were not an obvious deviation from the background. The peak recovery was not calculated for any run where 5000 kDa PEO was used as the coating polymer due to the possible inconsistency of user analysis. However, there was consistent activity detected around 3 and 5 minutes for short and long runs, respectively, as shown in Figure 12. Therefore, 5000 kDa PEO is not suggested as a polymer coating due to the atypical peak shape and significant user bias during analysis.

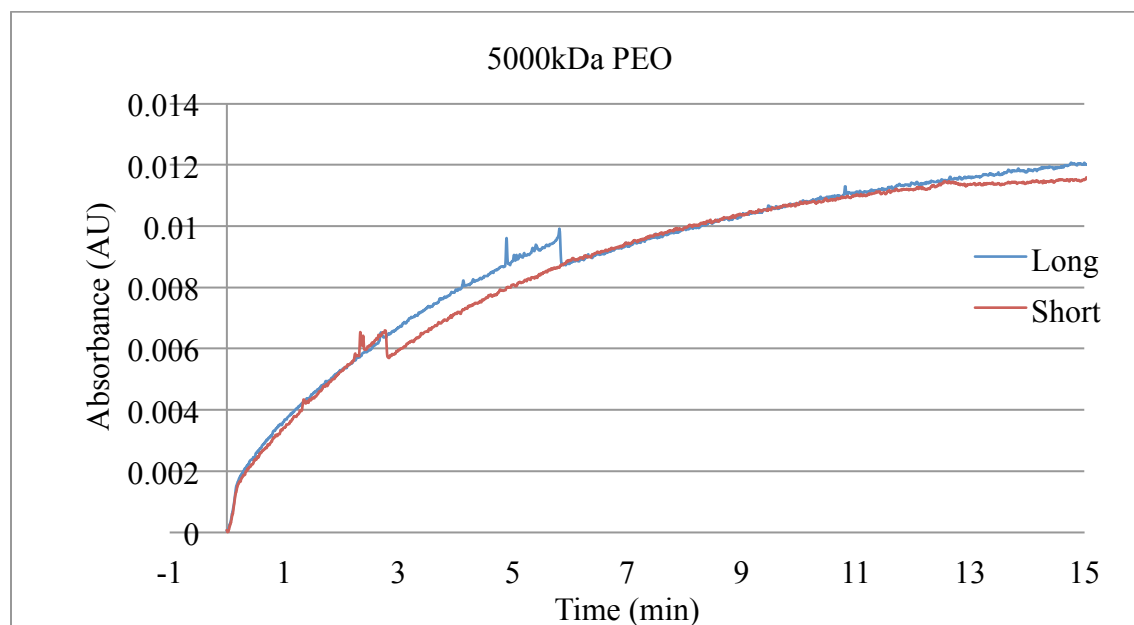


Figure 12: Representative electropherograms for a capillary coated with 5000 kDa PEO are shown. Typical bell shaped peaks did not occur, but every run had activity occurring around 3

minutes and 5 minutes for short and long runs, respectively.

### *8000 kDa PEO*

The representative electropherograms for a capillary coated with 8000 kDa PEO are shown in Figure 13. The peak recovery was largely askew for capillaries coated with 8000 kDa PEO. If the short runs detected a peak, it was around 5 and the long runs detected a large peak occurring around 10 minutes. Only two groups of long and short runs were possible due to the short runs not detecting  $A\beta_{1-42}$ . The average recovery was 1.4E5% with a standard deviation of 1.9E5%. This recovery is much larger than expected and results were largely varied. The extreme difference in peak areas could be due to the highly viscous nature of 8000 kDa PEO. Due to the viscosity, it is possible that the capillary was coated unevenly creating extreme error in the results. Furthermore, the short end of the capillary could have been coated very thickly and the long end of the capillary not coated at all. There is also a possibility that the PEO created a plug in the capillary and this contributed to the vastly different peak areas dependent on the run direction. Since the short end of the capillary was likely thickly coated, the protein had a much more difficult time navigating through the capillary to the detector, resulting in no detection. The long runs showed multiple peaks due to the fact that the farther end was hardly coated and the large peak was likely due to protein build up near the detector.

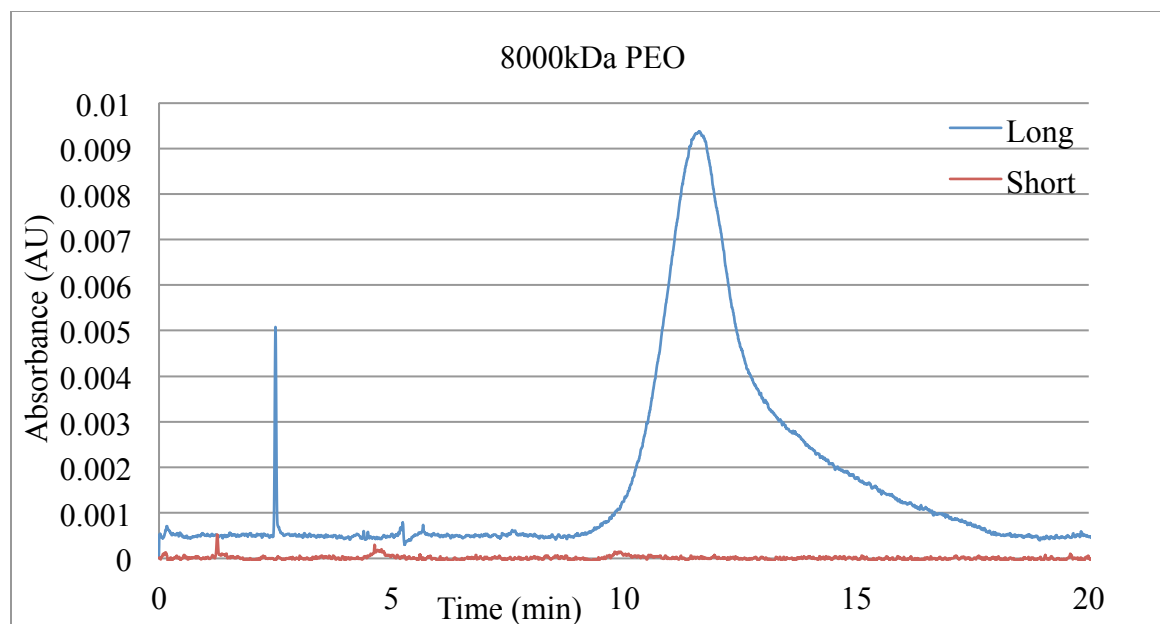


Figure 13: Representative electropherograms for a capillary coated with 8000 kDa PEO. The long runs showed a large peak starting around 10 minutes with a long tail. If the short runs detected a peak it was around 5 minutes.

#### 0.5% PVA

Polyvinyl alcohol was the only polymeric covalent coating analyzed. The exact molecular weight of PVA used to coat was difficult to determine since the coating process is more involved and the reaction occurs inside the capillary. Figure 14 shows representative electropherograms for the capillaries coated with 0.5% PVA. The two peaks compared were the short run around 25 minutes and the long run around 45 minutes. The peak recovery varied between the two capillaries tested. The average peak recovery for the first capillary was 64.3% +/- 49.1%. The average recovery was actually worse than that of an uncoated capillary. The second capillary had an average peak recovery of 1.8E4% with a standard deviation of 2.8E4%. Again, realistically a peak recovery greater than 100% is not valid. Due to the recovery inconsistency of  $A\beta_{1-42}$  when the capillary is coated with PVA, it was determined that PVA



would not be an acceptable polymeric coating in this instance.

However, theoretically, covalently coated capillaries last longer than dynamically coated capillaries. No experiments were performed to determine how many runs the 0.5% PVA coating lasted, but this could be a possible future study. For consistency, this may make 0.5% PVA a more attractive coating than 2000 kDa PEO since the protein recovery values are competitive.

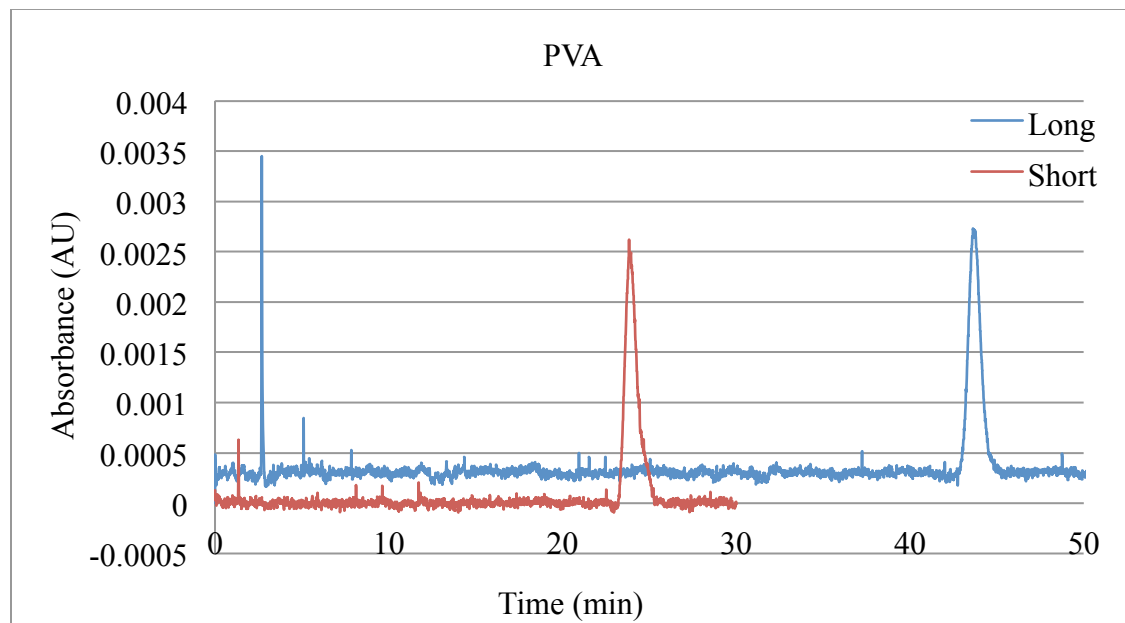


Figure 14: Representative electropherogram for a capillary coated with 0.5% PVA. The runs analyzed occurred around 25 minutes and 45 minutes, for the short and long runs, respectively.

### Overall Results

Overall, there is still a need to determine the best option for capillary coating to reduce  $A\beta_{1-42}$  loss when analyzing by CE. Recovery of  $A\beta_{1-42}$  on an uncoated capillary is between 65% and 70%. The best coating tested in this study was 2000 kDa with a recovery just under 90%, the protein recovery goal. The biggest issue with this study is a prominent recovery greater than 100%. It is still not fully understood why this issue is occurring, but it persists no matter the coating type. The most likely reasons for this issue are either a need for a better protein removal

rinse or an issue with the instrument sample injection due to an old pressure pump. Additionally, it should be pointed out that results vary depending upon the lot of  $A\beta_{1-42}$ .

## Chapter 3: Photo-Induced Cross Linking of Unmodified Proteins

### Introduction

Understanding how  $A\beta_{1-42}$  influences the degradation of neuronal cells requires knowledge of its formation including kinetics and structure. Due to the constantly evolving understanding of  $A\beta_{1-42}$  aggregation, it has been impossible to achieve a consensus among the scientific community. Cross-linking proteins could be a useful tool to understand the mechanisms in which proteins aggregate. However, current crosslinking methods have significant drawbacks of long reaction times with low yields.(30) Additionally, these crosslinking methods may require modifications of nucleophilic side chains and/or bifunctional crosslinkers, which have the potential to produce artificial results. An efficient and chemically inert method for crosslinking unmodified proteins, that occurs in less time than the protein takes to alter conformation, would be necessary to study this kind of interaction. The Kodadek laboratory at the University of Texas designed a light activated reaction capable of crosslinking proteins without modifying the protein prior to application. (30) This method, termed photo-induced crosslinking of unmodified proteins (PICUP), is about 60% efficient with a 0.5 second light exposure. PICUP was shown by Bitan et al. to efficiently and accurately capture transient oligomer species of  $A\beta_{1-40}$  by comparing the captured oligomer distribution to the oligomer distribution of native monomeric proteins and the distribution relationship to irradiation time. (20) Applying PICUP to  $A\beta_{1-42}$  at a fixed time interval during aggregation could help determine the size distribution and relative abundance of  $A\beta_{1-42}$  during the aggregation process.

PICUP is initiated by the light excitation of a tris(2,2'-bipyridyl)dichlororuthenium(II) complex which has a maximum UV absorption at 452 nm. (30) When Ru( II) is exposed to a short burst of light in the presence of an electron acceptor, such as ammonium persulfate (APS),

Ru (II) is oxidized to Ru (III). Ru (III) abstracts an electron from a nearby protein molecule regenerating Ru (II) and creating a protein radical. Ru (II) continues the cycle of protein radical formation until a reducing agent is added. This reaction is represented in Figure 15. The protein radical is free to attack a neighboring protein to form a covalent bond. Theoretically, the protein radical can form anywhere along the peptide chain. However, the radical preferentially forms at Tyr, His, or Met due to aromatic stabilization and neighboring group effects. (31) The primary factor to determine how the peptide is crosslinked is how close the radical is to a potential electron donor. The nature of the radical is unimportant because it will either be crosslinked or quenched by a solvent. (32) The use of long wavelength light is preferable because few molecules absorb outside the UV region, so PICUP could eventually be applied to living cells. In the absence of APS, the photoexcited Ru(III) generates a singlet oxygen. This reaction is about 20 fold less efficient and requires more light than PICUP with an electron acceptor. (30)

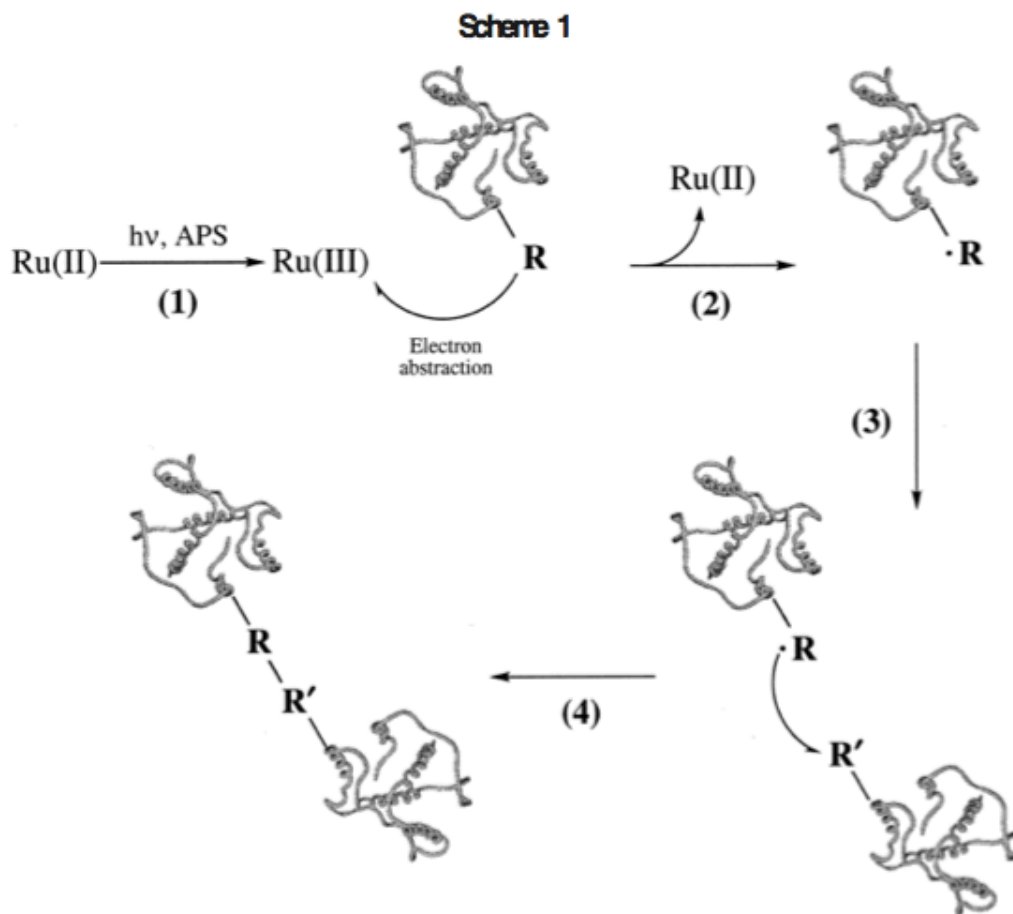


Figure 15: PICUP reaction scheme is shown starting with ruthenium being exposed to light in the presence of APS. A ruthenium(III) radical is then generated which extracts an electron from a neighboring residue. Ruthenium (II) is regenerated which can restart the process. The protein radical joins a neighboring protein residue and becomes cross-linked. The reactions is stopped by adding a reducing agent such as DTT or  $\beta$ -mercaptoethanol. Reprinted with permission from Bitan G, Teplow D. Rapid photochemical cross linking- a new tool for studies of metastable, amyloidogenic protein assemblies. *Accounts of Chemical Research*. 2004;37(6):357-64.

Copyright 2015. American Chemical Society.

PICUP is essential to studying A $\beta$  aggregation prior to SDS-PAGE analysis. Typically, protein complexes dissociate when treated with SDS so observation of larger assemblies under

native conditions cannot be detected via SDS analysis. Additionally, it has been demonstrated that SDS can artificially induce oligomerization of A $\beta$  and A $\beta$  can form SDS-stable oligomers. (11) Because A $\beta$  is an amphipathic protein, the protein is divided into SDS micelles, which causes a high concentration of monomer in the micelle and results in oligomerization. Therefore, A $\beta$  oligomer distributions shown via SDS-PAGE do not accurately reflect the native distribution. (33) It is necessary to covalently cross-link the oligomers so they are stable in the presence of SDS in order for this method to more accurately reflect the true aggregation species. (11)

PICUP samples have historically been analyzed by SDS-PAGE. However, SDS-PAGE only gives information about the relative molecular weight of samples present. Additionally, SDS denatures the protein as it travels down the gel and breaks down the protein's secondary and tertiary structure. A novel approach used in this study is to analyze PICUP samples using capillary electrophoresis (CE). CE separates proteins based on their size and charge. However, correlating individual peaks to a specific charge or size cannot be directly determined and therefore would require a model of the system. CE also allows the protein to remain in its native conformation as it is detected by UV light at 214 nm. By coupling SDS-PAGE and CE analysis, the limitations of both methods are counteracted and a plethora of information can be gained about the aggregation pathway of A $\beta_{1-42}$ .

Bitan et al. successfully applied PICUP and densitometrics with AB $_{1-42}$  and found that oligomers preferentially exist in pentamer/hexamer units rather than monomers. (34) The three distinct groups of aggregate-free A $\beta_{1-42}$  oligomers were found to be: monomer through trimer, tetramer through octamer, and dodecamer through octadecamer. Monomer through trimer showed decreasing intensity as higher order oligomers were formed. Tetramer through octamer showed a Gaussian-like distribution with the maximum occurring at pentamer/hexamer. The

intensity of the bands correlating to higher order oligomers seemed to form from self-association with pentamer/hexamer units. (34) The A $\beta_{1-42}$  assembly studied by Bitan et al consisted of aggregate free samples. In this study, PICUP will be applied to A $\beta_{1-42}$  samples at distinct time points after inducing aggregation to deduce the size of A $\beta_{1-42}$  species along the aggregation pathway.

Ultimately, the experimental data correlating the molecular weight and electrophoretic mobility via SDS-PAGE and CE, respectively, will be used as a basis for a computational model that has the ability to more rapidly analyze the size and concentration of A $\beta_{1-42}$  present in a sample. The molecular weight determined by SDS-PAGE analysis shows roughly the size of the species present, but not the exact molecular weight. Therefore, there is a need for a model that can predict the molecular weight of the species present based on the electrophoretic mobility provided by CE (or ME) analysis.

The electrophoretic mobility can be calculated by the following equation:

$$\mu = \frac{L_t L_d}{t_m V} \quad (3)$$

where  $L_d$  is the length of the capillary to the detector,  $L_t$  is the total length of the capillary,  $t_m$  is the migration time of the protein, and  $V$  is the applied voltage. The extended Ogston model correlates the electrophoretic mobility in a sieving matrix to the electrophoretic mobility in buffer solution by:

$$\log(\mu) = \log(\mu_o) - K_R \Phi \quad (4)$$

where  $\mu$  is the sieving electrophoretic mobility,  $\mu_o$  is the buffer electrophoretic mobility,  $K_R$  is the protein retardation coefficient, and  $\Phi$  is the polymer concentration (weight percent). A Ferguson plot ( $\log(\mu / \mu_o)$  vs.  $\Phi$ ) is used to determine the protein retardation coefficient, where

the slope is negative  $K_R$ . The protein retardation coefficient relates to the radius of the protein by:

$$K_R = \pi l' (r + R)^2 \times 10^{-16} \quad (5)$$

where  $l'$  is the total length of the polymer fiber per unit volume,  $r$  is the polymer fiber radius,  $R$  is the protein radius. Multiangle light scattering (MALS) can be used to determine the polymer fiber radius and the protein radius. It can be assumed that the  $A\beta_{1-42}$  aggregate radius is an effective radius since the aggregate may or may not be spherical. Once the radius is determined, the molecular weight can be related to the radius by:

$$R_M = \left( \frac{3 V_M M_w}{4 \pi N} \right)^{1/3} \times 10^7 \quad (6)$$

where  $R_M$  is the effective radius,  $V_M$  is the partial specific volume,  $M_w$  (Da) is the molecular weight, and  $N$  is Avogadro's number. The MATLAB code for this simulation can be viewed in the Appendix.

## **Materials and Methods**

### *Amyloid beta preparation*

Amyloid beta 1-42 (Anaspec, Fremont CA, Lot #1360300), was stored at  $-80^\circ\text{C}$ . To ensure samples were monomeric, a 1 mg/mL stock of amyloid beta was prepared in Hexafluoro-2-propanol (HFIP). Amyloid beta was aliquotted into vials containing 0.0271 mg and the HFIP was allowed to evaporate in the hood overnight. The amyloid beta was brought up to an initial concentration of 20  $\mu\text{M}$  with 5 mM NaOH and 10 mM phosphate buffer.

### *PICUP*

Photo-induced cross-linking of unmodified proteins was performed using a Carl Zeiss Xenon arc lamp XBO 75W/2 with power supply model #910135, 120V/120W, 50W HBO/75W



XBO. The camera used was a Mamiya/Sekor 500 DTL. The camera was interfaced with a 9.875 inch cardboard tube to ensure the camera remained a constant distance from the Xenon lamp. Light exposure was controlled with a shutter setting of 1 second. No filter was used to filter the light. The reaction was performed in a dark room. The protocol was developed based on Bitan et al. with modifications as described below. (33) Bitan et al. successfully used a 1:2:40 A $\beta$ :Ru:APS mol ratio and 1 second of light exposure to capture A $\beta$  oligomeric species. In order to capture A $\beta$  oligomeric species in the Hestekin laboratory, a 1:500:10000 A $\beta$ :Ru:APS mol ratio and 1 second of light exposure was used.

Final concentration of .033mM A $\beta$ <sub>1-42</sub> was added to 0.5 mL non-stick eppendorf tubes followed by 1.67 mM Ruthenium and 33.3 mM Ammonium Persulfate (APS), all dissolved in 10mM phosphate buffer. Once APS was added to the reaction mixture, the tube was quickly placed in front of the camera lens, perpendicular to the beam of light, and exposed to 1 second of light by pressing the camera shutter. The reaction was quickly quenched with 5%  $\beta$ -mercaptoethanol and placed in the -80°C freezer. All PICUP samples analyzed via capillary electrophoresis were done so on a capillary coated with 2000 kDa PEO. The sample was electrokinetically injected for 15 s and separated at 7 kV for 30 minutes with a 0.17 min ramp. No polymer matrix was used for separation. PICUP samples analyzed via SDS-PAGE were run on a 12% Tris-glycine gel to analyze higher molecular weight species or on a 16.5% Tris-tricine gel to analyze lower molecular weight species. Each gel was run for 2.5 hours at 100 V with 20  $\mu$ L of sample per well. GE Healthcare Life Sciences PlusOne Protein Silver Staining Kit was used to stain the SDS-PAGE gels.

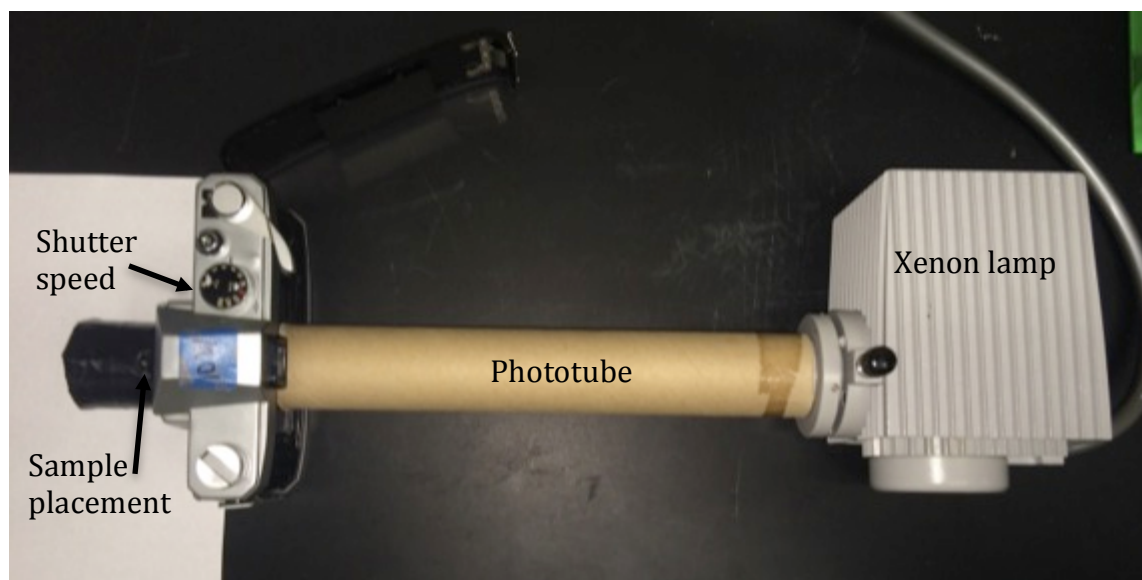


Figure 16: The photo-system used for performing PICUP on  $A\beta_{1-42}$ . The eppendorf tube containing the sample is placed in a small hole right in front of the camera. The amount of light exposed to the sample is controlled by the shutter speed. The phototube keeps the sample 9.875 inches from the Xenon lamp. This is estimated to be about 75 Joules of light.

### *Data Analysis*

Capillary electrophoresis data was analyzed using Origin 9.0 and Microsoft Excel. The data was imported into Origin where the baseline was subtracted by user identification. The peaks were fit with a bigaussian curve. The area under the bigaussian curve was calculated by “Peak Analyzer” using the Origin software. The data was copied into excel where it was plotted versus time. Gels were scanned with an Epson scanner at 600 dpi.

### **Results and Discussion**

Bitan et al. successfully used a 1:2:40  $A\beta$ :Ru:APS mol ratio and 1 second of light exposure to capture  $A\beta$  oligomeric species.(33) After PICUP application,  $A\beta_{1-42}$  showed a ladder

of bands ranging from molecular weight 4.2 kDa to 55.4 kDa via SDS-PAGE and silver staining analysis. Without light irradiation,  $A\beta_{1-42}$  had two bands around 4 kDa and 14 kDa (monomer and trimer). Bitan's results are shown in Figure 17 and were used as the Hestekin's lab standard for success.

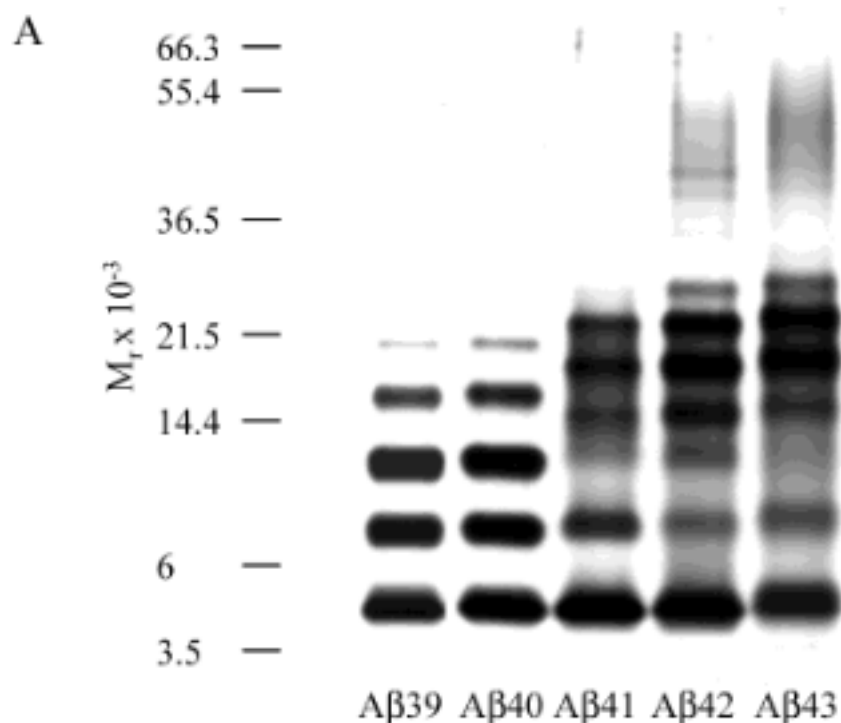


Figure 17: Example of the ladder-like distribution seen by Bitan et al. for  $A\beta$  with a different C-terminus after applying PICUP. The ladder-like distribution is what the Hestekin lab considered to be a successful application of PICUP to  $A\beta$ . Reprinted with permission from Bitan and Teplow (2004). Rapid photochemical cross linking- a new tool for studies of metastable, amyloidogenic protein assemblies. *Accounts of Chemical Research*. 2004;37(6):357-64.

Copyright 2015. American Chemical Society

The ratio used by Bitan et al. was repeatedly unsuccessful in the Hestekin laboratory. A study was conducted to optimize the oligomeric A $\beta_{1-42}$  capture by increasing the ratio of reactants to A $\beta_{1-42}$ . Table 3 describes this study and the results are presented in Figure 18.

Table 3: Optimization of PICUP reaction for A $\beta_{1-42}$  by varying the molar ratio of the reactants. All values of reactants given are the final concentration in mM. The quench agent,  $\beta$ ME, must be added in 1:1 ratio to the amount of sample. Samples 1 and 2 are similar to the experiment performed by Bitan et al.

Sample	A $\beta_{1-42}$ (mM)	Ru(bpy) <sub>3</sub> (mM)	APS (mM)	Light (sec)	A $\beta$ : Ru(bpy) <sub>3</sub> : APS
1	0.018	0.050	1.000	0	1:2.78:55.6
2	0.018	0.050	1.000	1	1:2.78:55.6
3	0.016	0.091	1.818	0	1:5.56:111.1
4	0.016	0.091	1.818	1	1:5.56:111.1
5	0.007	0.333	6.667	0	1:50:1000
6	0.007	0.333	6.667	1	1:50:1000
7	0.007	3.333	66.667	0	1:500:10000
8	0.007	3.333	66.667	1	1:500:10000

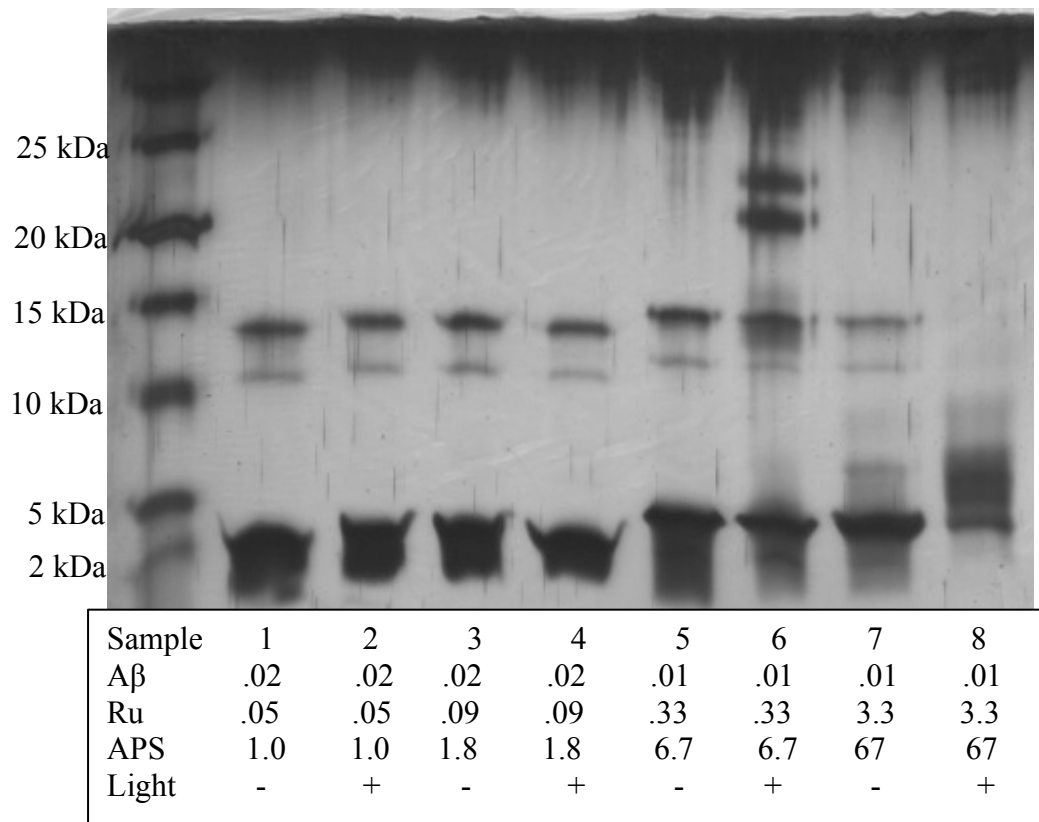


Figure 18: Results from the optimization of PICUP reaction. Samples 1 and 2 are of Bitan et al. concentrations. Considering the reaction looks the same with and without light, protein capture was not successful. However, increasing the reactants amounts 180-fold to Aβ produce the appropriate results, as seen in sample 8. The final concentrations of each reactant are displayed in Table 1.

Samples 1 and 2 are similar to the molar ratio used by Bitan et al. for Aβ<sub>1-40</sub>. Samples 3 and 4 double the reactant to Aβ<sub>1-42</sub> ratio. Samples 5 and 6 contain almost an 18-fold increase in the molar ratio of reactants to Aβ<sub>1-42</sub>. Samples 7 and 8 contain almost an 180 fold increase of Ru(bpy)<sub>3</sub> and APS to Aβ<sub>1-42</sub>. Figure 18 displays the ladder-like distribution of Aβ of varying lengths after applying PICUP reported by Bitan et al.

As seen in samples 1-4 of Figure 17, the molar ratio used by Bitan et al. and an excess of that used by Bitan et al. were unsuccessful in capturing the oligomeric  $A\beta_{1-42}$  species as it does not show the reported ladder like distribution. Additionally, the samples that were exposed to light look identical to the samples that were not exposed to light, suggesting that irradiation by light did not occur. Samples 5 and 6 contain an almost 18-fold increase in reactant ratio. Sample 5 was not exposed to light and looks identical to samples 1 through 4. However, when the same sample (sample 6) is exposed to one second of light, additional bands are shown between 20 and 25 kDa. Increasing the ratio 10-fold more, sample 7 looks similar to samples 1 through 5 and was not exposed to Xenon light. Sample 8 shows the ladder distribution of  $A\beta$  reported by Bitan et al. and resulting in an effectively photo-crosslinked  $A\beta$ . A few ladder species are seen in sample 7 when no Xenon light is applied to the sample. This is likely due to unavoidable arbitrary light. Interestingly, for samples 1 through 5 where PICUP was not successful, three bands were identified: one band between 2 and 5kDa and two bands between 10 kDa and 15 kDa. This directly correlates to  $A\beta$  samples taken from the temporal cortex of patients with AD and detected via immunoprecipitation/western blotting. (6) The specific reported molecular weight of these bands was 4.1 kDa, 7.5 kDa, and 12.1 kDa. This further confirms the need to use PICUP to accurately visualize the  $A\beta$  species present in a sample.

After the appropriate molar ratio of reactants was determined, the validity of each reaction component in the PICUP procedure was tested and analyzed on a 16.5% Tris-tricine gel to observe that each reactant is needed for the reaction to proceed optimally. These results are shown in Figure 19. Additionally, it was important to determine if the reaction would proceed with minimal (or no) use of a reactant as the more reactants used, the higher the chances for

interference with CE detection. All samples were quenched with 5%  $\beta$ -Mercaptoethanol at a 1:1 ratio to the sample amount. Each sample alternated no light and 1 second of light exposure. Samples 1 and 2 contain no A $\beta$  and therefore no protein bands. Samples 3 and 4 contain no Ruthenium, and 3 strong bands around 3, 10, and 13 kDa. Samples 5 and 6 contain no APS. Sample 5 has the same bands as the samples containing no Ruthenium. Sample 6, however, shows a ladder of bands. This supports the claim that Ruthenium generates a singlet oxygen in the absence of APS and the presence of light due to the fact that the ladder of bands are weaker than in the presence of APS. Samples 7 and 8 contain no Ruthenium or APS and display the same bands as lanes 4-7. Sample 9 contains all reactants and has the strongest ladder of bands. It is obvious that in the absence of APS (sample 6) crosslinking is not as efficient as in the presence of the electron acceptor (sample 9) because the intensity and amount of the bands are decreased.

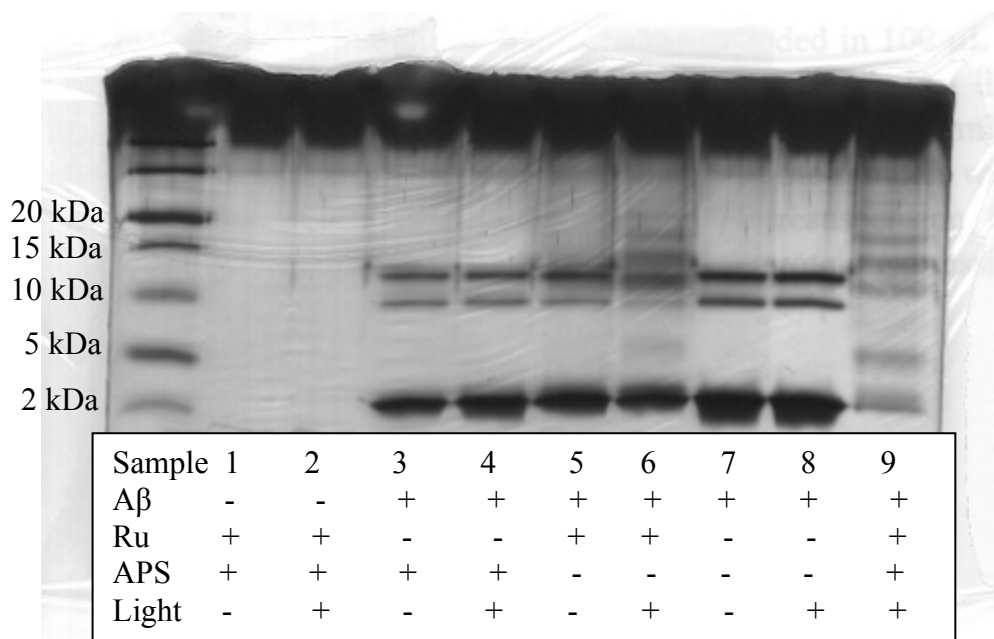


Figure 19: An experiment confirming the validity of the PICUP reaction by sequentially testing the importance of each reaction component for capturing oligomeric species of  $A\beta_{1-42}$  and running the samples on a 16.5% Tris tricine gel. Each lane alternates no light and 1 second of exposure. The lane containing  $A\beta$ , Ru, APS, and 1 second of light shows the most distinct ladder of  $A\beta_{1-42}$  species.

Once the correct reactant ratio was determined,  $A\beta_{1-42}$  was aggregated at 800 rpm for 2 hours. A sample was taken every 15 minutes and subjected to PICUP. The results are shown in Figure 20. At every time point, a ladder of protein sizes are present. At 0 minutes of aggregation, the majority of the protein detected is between 2 kDa and about 8 kDa. At 120 minutes, the majority of the protein detected is between 2 kDa and 5 kDa. The amount of protein in each lane gradually decreases as time progresses, suggesting that very large aggregates are being made and likely caught at the top of the gel.

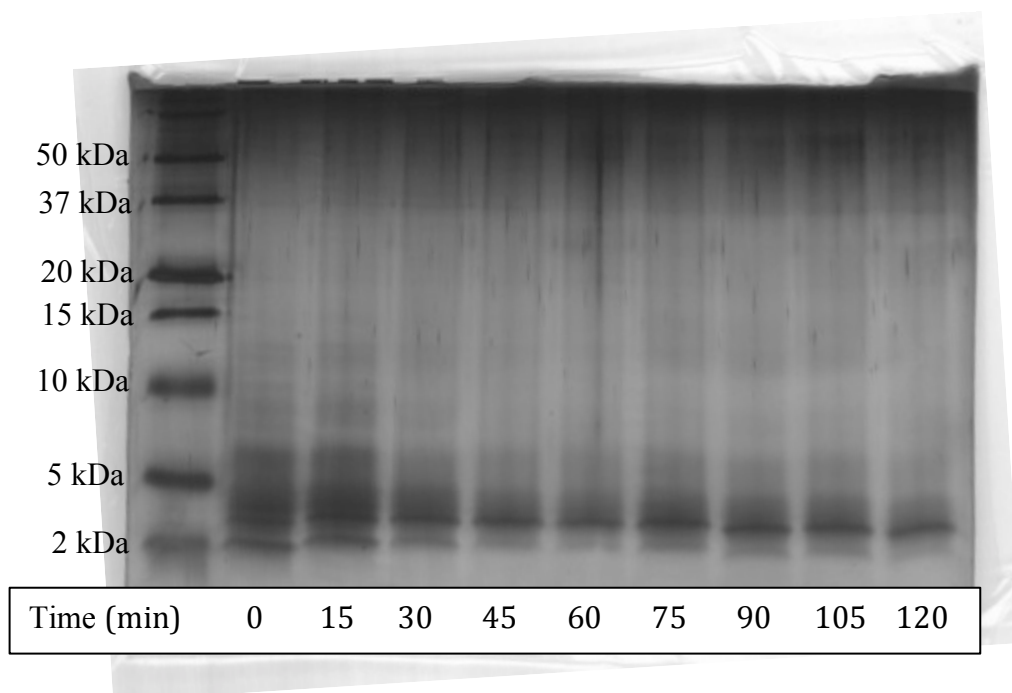




Figure 20:  $A\beta_{1-42}$  aggregated at 800 rpm subjected to PICUP analyzed on a 16.5% Tris-tricine gel. The left most lane contains protein molecular weight standards. Each following lane analyzes the time of aggregation prior to PICUP.

In order to detect the higher molecular weight species formed after two hours of aggregation, PICUP was analyzed on a 12.5% Tris-glycine gel. Results are shown in Figure 20. Similar to the 16.5% Tris-tricine gel, the majority of protein detected is found between 2 kDa and 8 kDa at 0 minutes to 2 kDa and 5 kDa at 120 minutes. No additional higher molecular weight species were found when compared to the 16.5% Tris-tricine gel. It is possible that after two hours of aggregation,  $A\beta_{1-42}$  species has a molecular weight higher than 50 kDa and bands exist that are not seen. This could be tested by running the gel for longer than 2.5 hours and possibly letting the smaller molecular weight bands to travel off of the gel. Also, the samples could be analyzed with CE and to see if peaks come out after the normal run time of 30 minutes.

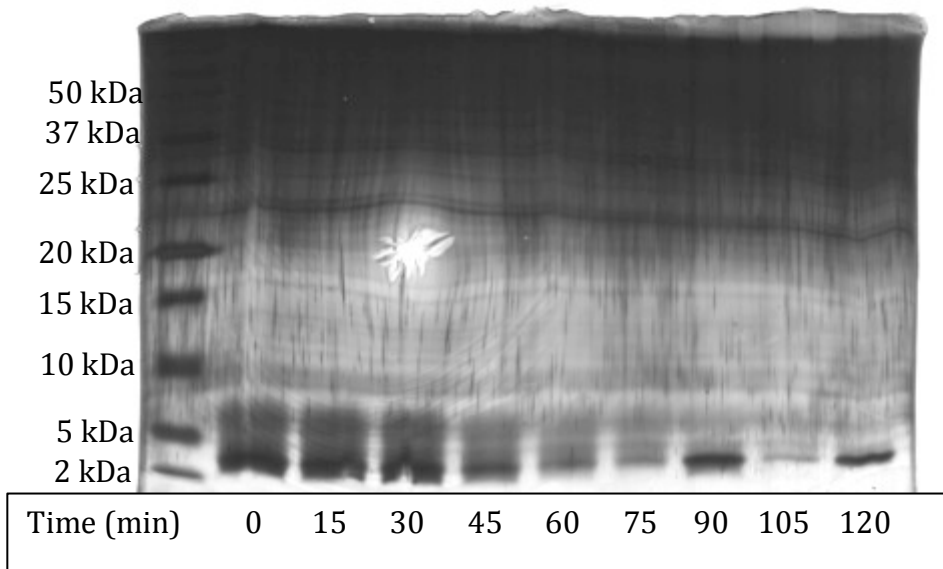


Figure 21: A $\beta_{1-42}$  aggregated at 800 rpm subjected to PICUP analyzed on a 12.5% Tris-glycine gel. The left most lane contains protein molecular weight standards. Each following lane analyzes the time of aggregation prior to PICUP. The higher molecular weight species are more separated in the 12.5% Tris-glycine gel versus the 16.5% Tris-tricine gel. Therefore, this gel should more optimally show higher molecular weight species.

In order to analyze the samples via CE, control samples containing each reactant at the appropriate final concentration were run to ensure no reactant absorbs UV light at 214 nm and causes interference for detecting the protein. Since the final concentration of A $\beta_{1-42}$  is low (3.33  $\mu$ M), the protein must be electrokinetically injected for 15 seconds, which preferentially injects charged groups into the capillary to be detected. Figure 22 shows the results of electrokinetically injecting Ruthenium, APS, Co(III), Dithiothreitol (DTT), and 5%  $\beta$ -Mercaptoethanol separately.

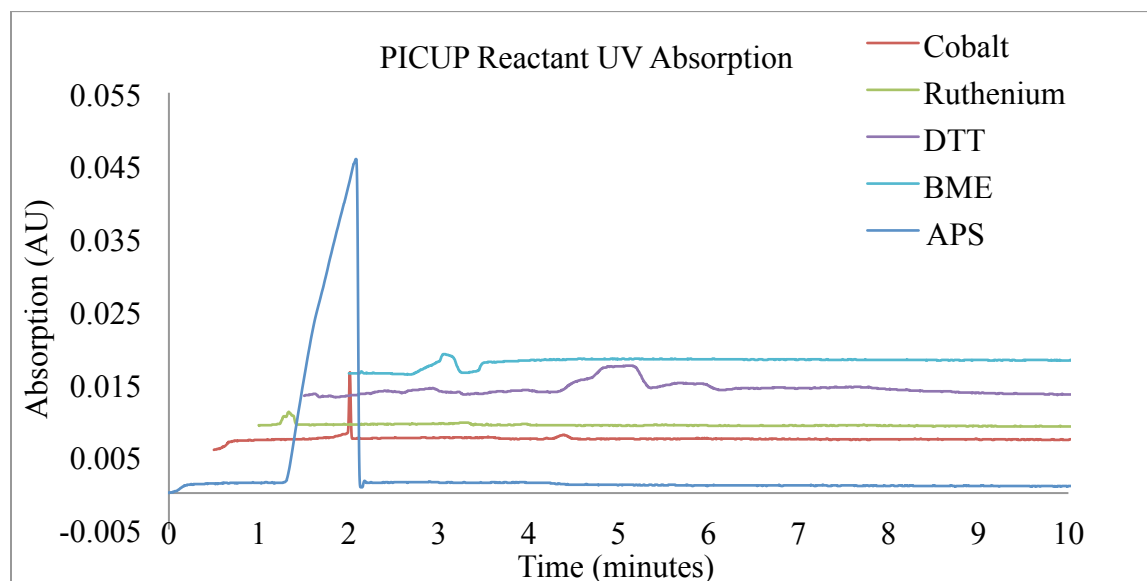


Figure 22: All potential PICUP reactants are shown in the above electropherogram. All reactants relate to the vertical axis on the left except APS. Ruthenium does not absorb UV light at 214nm. The potential electron acceptors, APS and Cobalt (III), both absorb UV light. APS

creates a peak around 2.5 minutes that masks  $A\beta_{1-42}$  oligomers. Cobalt portrays multiple peaks. The potential quenching agents,  $\beta$ -Mercaptoethanol and DTT, create noisy data and are unusable in samples to detect  $A\beta_{1-42}$  oligomers.

Ruthenium does not absorb UV light at 214 nm and is acceptable to use in samples with  $A\beta_{1-42}$ . The electron acceptor, APS has a predictable peak that is detected around 2.5 minutes. However, the location of this peak masks oligomeric  $A\beta_{1-42}$  species, so it would be beneficial to remove APS. Therefore, a Co (III) solution was tested as a potential electron acceptor instead of APS. Co (III) was chosen as an alternative electron acceptor because it is a water-soluble metal ion complex willing to donate an electron under the correct conditions.(35) Vollers et al. performed PICUP reactions with  $A\beta_{1-42}$  and noted that Co (III) could be a possible alternative. The efficiency of Co (III) as a potential electron acceptor was tested by performing a PICUP experiment and replacing the APS with Co (III) and analyzing the samples on a 16.5% Tris tricine gel, these results are shown in Figure 23. Additionally, Co (III) was electrokinetically injected to test its UV absorption at 214 nm, these results are shown in Figure 22.

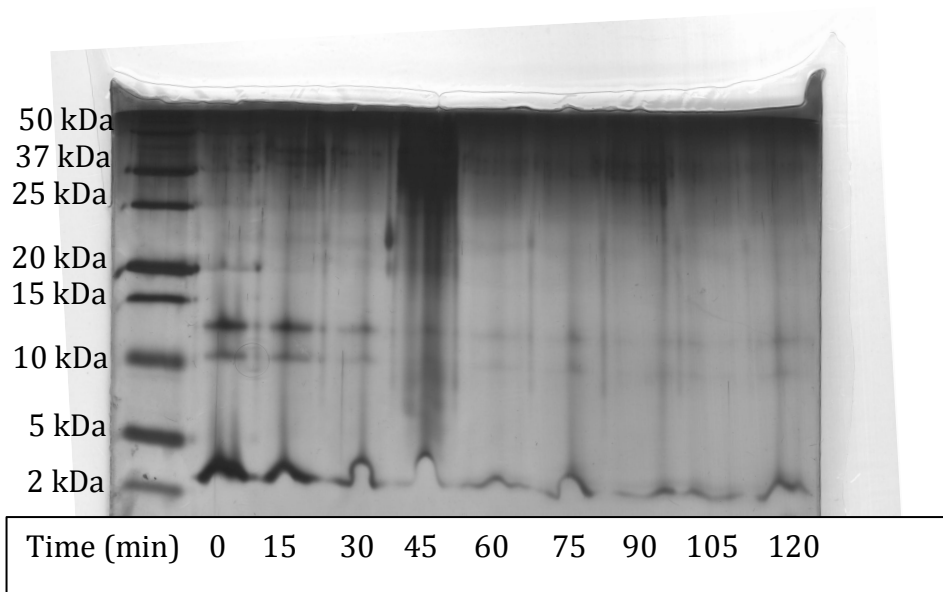


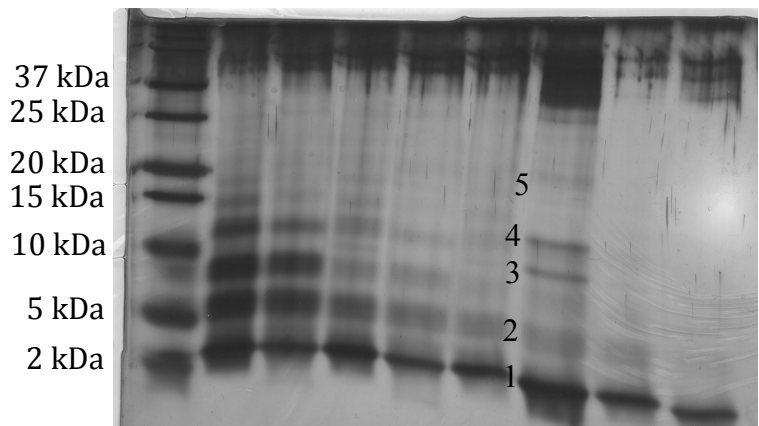
Figure 23: A $\beta_{1-42}$  aggregated at 800 rpm subjected to PICUP using Co(III) rather than APS as an electron acceptor and analyzed on a 16.5% Tris-tricine gel. The left most lane contains protein molecular weight standards. Each following lane analyzes the time of aggregation prior to PICUP.

Comparing Figure 23, which uses Co (III) as an electron acceptor, and Figure 20, which uses APS as an electron acceptor, it is clear that APS captured more transient species of A $\beta_{1-42}$  by the number of bands represented on the gel. Additionally, the Co (III) would not stay in solution, causing the band between 2 and 5 kDa to have a wavy effect. Co (III) was also analyzed by CE to determine if it absorbs light at 214 nm at the appropriate concentration. Looking at Figure 22, it is clear that Co (III) does absorb UV light by the peak around 2 minutes. Therefore, Co (III) was determined to not be an acceptable alternative electron acceptor in PICUP applications with A $\beta_{1-42}$ . No other electron acceptors were tested.

Additionally, both quenching agents greatly interfere with protein detection.  $\beta$ -Mercaptoethanol and DTT create noisy data and their presence in samples after PICUP inhibits the ability to precisely detect protein using CE over the entire time period of detection. In order to detect A $\beta_{1-42}$  PICUP samples on via CE,  $\beta$ -Mercaptoethanol and DTT should not also be present in the sample. No other quenching agents were tested.

In order to overcome the inability of PICUP agents to be used in A $\beta_{1-42}$  samples for CE analysis two methods were tested. The first method used 2000 kDa filters and 100 mM phosphate for dialysis, similar to the separation conditions using CE. The filter size of 2000 kDa was chosen due to the large discrepancy between the molecular weight of A $\beta_{1-42}$  and the PICUP

reagents.  $A\beta_{1-42}$  has a molecular weight of 4514.06 Da; APS, Ruthenium, and  $\beta$ -Mercaptoethanol have molecular weights of 228.18 g/mol, 748.62 g/mol, 78.13 g/mol, respectively. A 2000 kDa filter was considered an appropriate size to release the reagents while retaining  $A\beta_{1-42}$ . The PICUP reaction proceeded as follows: 4  $\mu$ L of 20  $\mu$ M  $A\beta_{1-42}$  was added to 4  $\mu$ L of 200  $\mu$ M APS and 4  $\mu$ L of 10  $\mu$ M Ruthenium then subjected to 1 second of Xenon light. Afterwards, the reaction was quenched with 12  $\mu$ L of 5%  $\beta$ -Mercaptoethanol in 10 mM phosphate buffer. The sample was then allowed to filter through a 2000 kDa membrane for 24 hours. The phosphate buffer was changed every two hours for the first 10 hours then left overnight. Figure 24 shows the resulting Tris-tricine gel for dialysis samples and Figure 25 shows CE analysis for dialysis samples. Figure 26 shows a closer view of Figure 25.



Sample	1	2	3	4	5	6	7	8
Time	0	0	45	45	75	75	120	120
Dialysis	-	+	-	+	-	+	-	+

Figure 24: Samples 1, 3, 5, and 7 are PICUP samples that did not undergo dialysis. Samples 2, 4, 6, and 8 did undergo 24 hours of dialysis to remove the APS and 5%  $\beta$ -Mercaptoethanol. The lanes that underwent dialysis show some protein loss, but dialysis did not alter the conformation captured during PICUP.

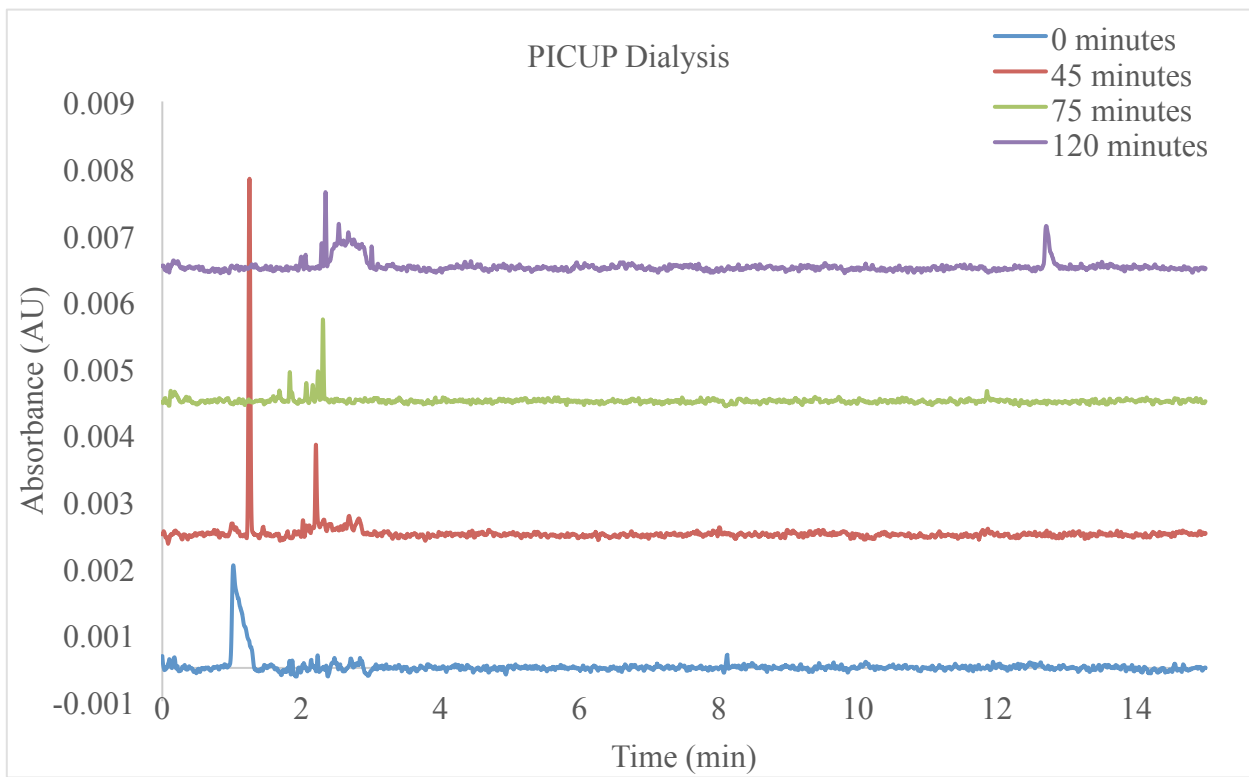


Figure 25: The aggregation pathway of  $A\beta_{1-42}$  analyzed via CE after a 2 hour aggregation at 800 rpm and 24 hours of dialysis to remove APS and 5%  $\beta$ -Mercaptoethanol. Generally, more species are present after more aggregation.

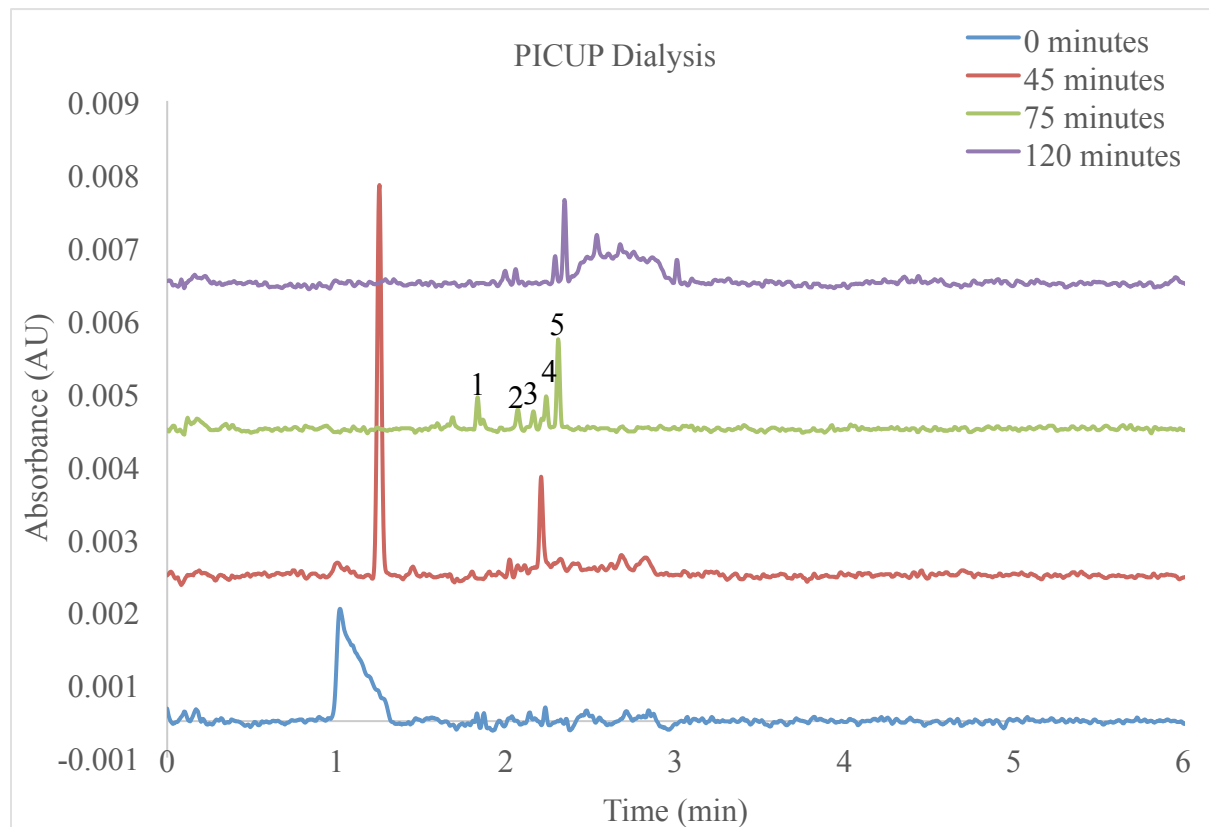


Figure 26: The aggregation pathway of  $A\beta_{1-42}$  analyzed via CE after a 2 hour aggregation at 800 rpm and 24 hours of dialysis to remove APS and 5%  $\beta$ -Mercaptoethanol. This is the same data as Figure 25, but with a closer view of initial peaks detected by CE.

Figure 24 shows that dialysis does not alter the  $A\beta_{1-42}$  conformation captured using PICUP because the same bands are present in each sample taken at the same time point. However, the bands for samples 2, 4, 6, and 8 are not as intense, showing protein loss during

dialysis. Figure 25 shows that the majority of APS and 5%  $\beta$ -Mercaptoethanol appears to have been successfully removed using dialysis since the peaks present in the samples do not correlate with the individual reagents (Figure 22). However, Figure 26 shows that there does seem to be residual APS in the 0 minute aggregation sample and residual  $\beta$ -Mercaptoethanol in the 120 minute aggregation sample. Therefore, the dialysis procedure could use some further modification to achieve greater consistency of maximizing protein retention and reactant loss across samples. Figure 26 also shows that the longer  $A\beta_{1-42}$  is aggregated, the more distinct species are present. These peaks mainly elute between 2-4 minutes. From Figure 26, it looks as if the 0 minutes sample still contained residual APS given the large peak at 1 minute. For this sample, dialysis was not as efficient since the other samples do not contain this peak. For 0 minutes, it is likely that APS is masking the  $A\beta_{1-42}$  and real peaks of monomeric protein cannot be seen. The 45 minute, 75 minute, and 120 minute samples all have a strong consistent peak after 2 minutes. Similarly, the same samples have a strong, consistent band between 2 and 5 kDa. It is hypothesized that the peak eluted after 2 minutes correlates with the first band in each sample. The 45 minute sample has a strong peak just after 1 minute that is not located in any other sample. There are no definite conclusions able to be drawn from which band this could correlate to since there are many bands that are stronger in the 45 minute sample than the 75 minute and 120 minute, and the 0 minute CE sample is not a credible reference. It looks as though dialysis was most efficient for the 75 minute sample due to the sharp separation of peaks. The 5 peaks shown for the 75 minute sample could correlate to the 5 bands shown on the gel. The 120 minute sample additionally looks as though dialysis wasn't as efficient due to the large wide peak before 3 minutes. This could be caused by residual  $\beta$ -Mercaptoethanol. The  $A\beta_{1-42}$  detection via CE was heavily dialysis dependent, as seen by the differences in the 0 minute and



75 minute samples. This experiment was repeated twice more, but as the samples within this experiment relied heavily on dialysis efficiency, the other results did as well. This caused the results to not be consistent within each time point or within each experiment. However, as seen from the 75 minute sample, dialysis could be a promising method to removing the PICUP reagents and detecting  $A\beta_{1-42}$  if the procedure could be made more consistent.

The second method used to detect  $A\beta_{1-42}$  via CE analysis without interfering PICUP reactants involved removing APS and  $\beta$ -Mercaptoethanol completely.  $A\beta_{1-42}$  was subjected to Ruthenium and light, then quenched by freezing the sample at  $-80^{\circ}\text{C}$ . No electron acceptor or chemical quenching agent was used. This means an oxygen radical was generated in the PICUP reaction and subsequently only the most easily oxidized species were cross-linked.

Shown in Figure 27, a 16.5% Tris-tricine gel was used to analyze PICUP without APS. A ladder of protein bands was not shown after silver staining. The band locations are identical to the locations in Figure 19, when APS is not present and in Figure 18 using the unoptimized PICUP reagent ratio. However, taking into account the results from CE (Figures 28 and 29) as described below, it is possible that the PICUP reaction occurred, but not as efficiently as it would have in the presence of APS.

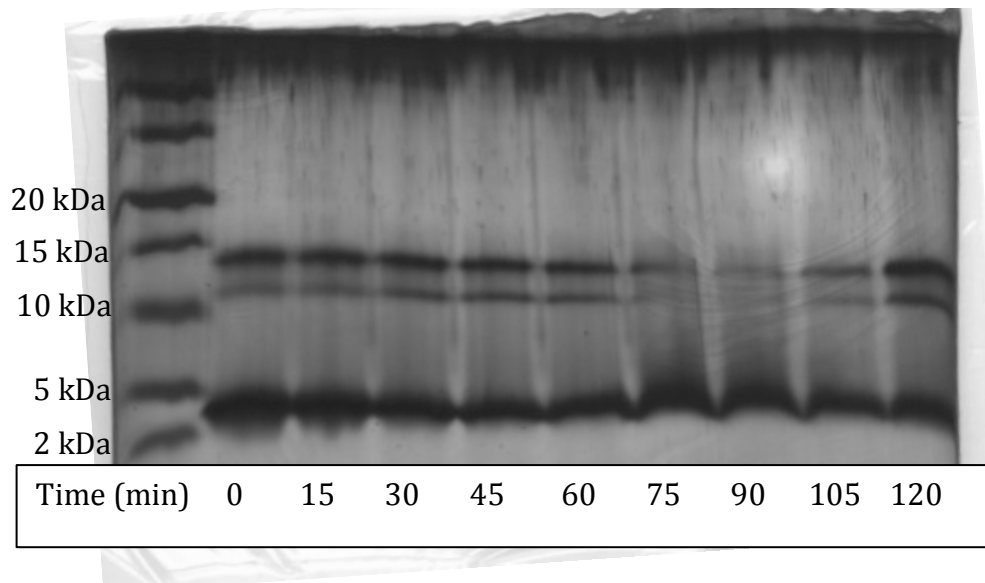


Figure 27:  $A\beta_{1-42}$  aggregated at 800 rpm subjected to PICUP without APS analyzed on a 16.5% Tris-tricine gel. The left most lane contains protein molecular weight standards. Each following lane analyzes the time of aggregation prior to PICUP.

Figures 28 and 29 display the same samples as Figure 26 analyzed by capillary electrophoresis. Figure 28 displays there are a multitude of peaks between 0 and 4 minutes. Figure 29 shows a closer look at the species detected between 0 and 4 minutes. At 0 minutes, there is one large peak just before 2 minutes. This peak grows until the 60 minute sample, where it is absent and replaced by four smaller peaks. The four smaller peaks become six small peaks in the 75 minute sample. The six small peaks become three larger peaks in the 90 minute sample. After 90 minutes, the peaks grow in area until 120 minutes. No testing was done after 120 minutes of aggregation. The samples analyzed by CE and a Tris-tricine gel, Figures 27 and 28 respectively, do not correlate. This could be due to the fact that CE is more sensitive and has a lower limit of detection than Tris-tricine gels.

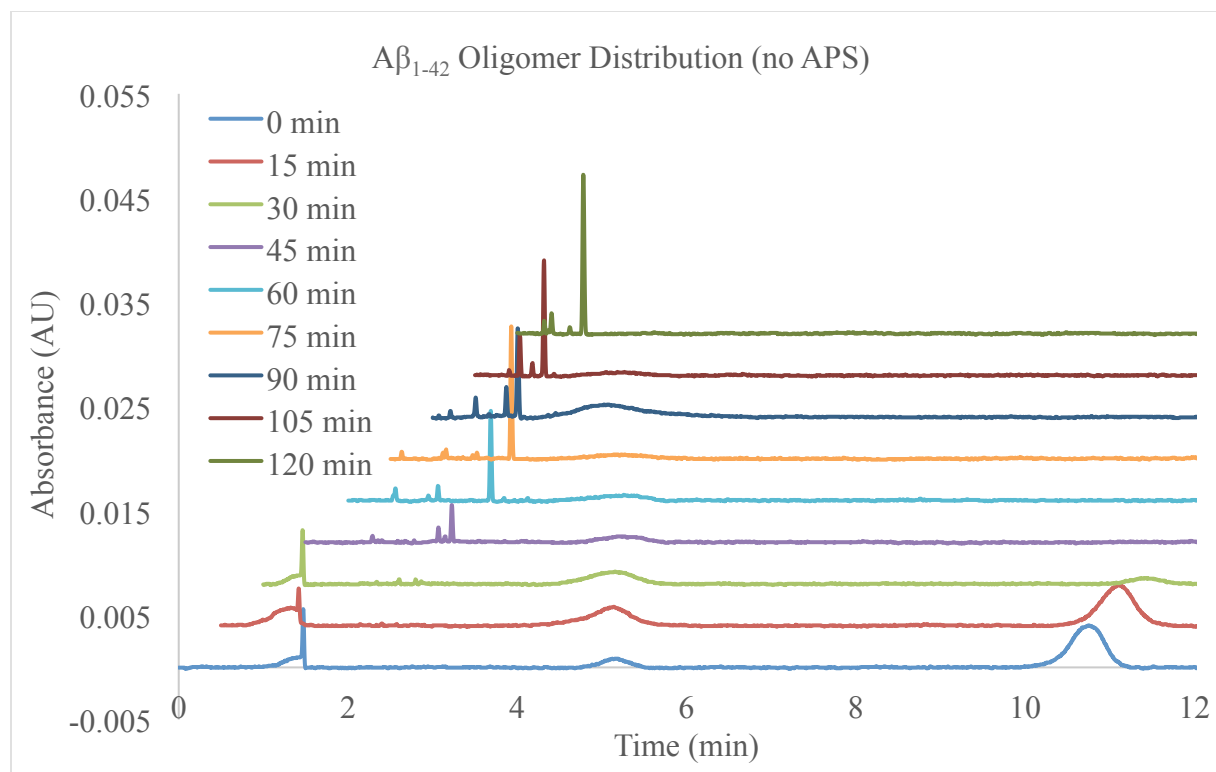


Figure 28: A $\beta_{1-42}$  was aggregated at 800 rpm for 2 hours. A sample was taken every 15 minutes and subjected to Ru(bpy)<sub>3</sub> and 1 second of Xenon light. The reaction was quenched by placing the sample in the freezer. Each sample was analyzed by CE. Each peak corresponds to protein detection at 214 nm.

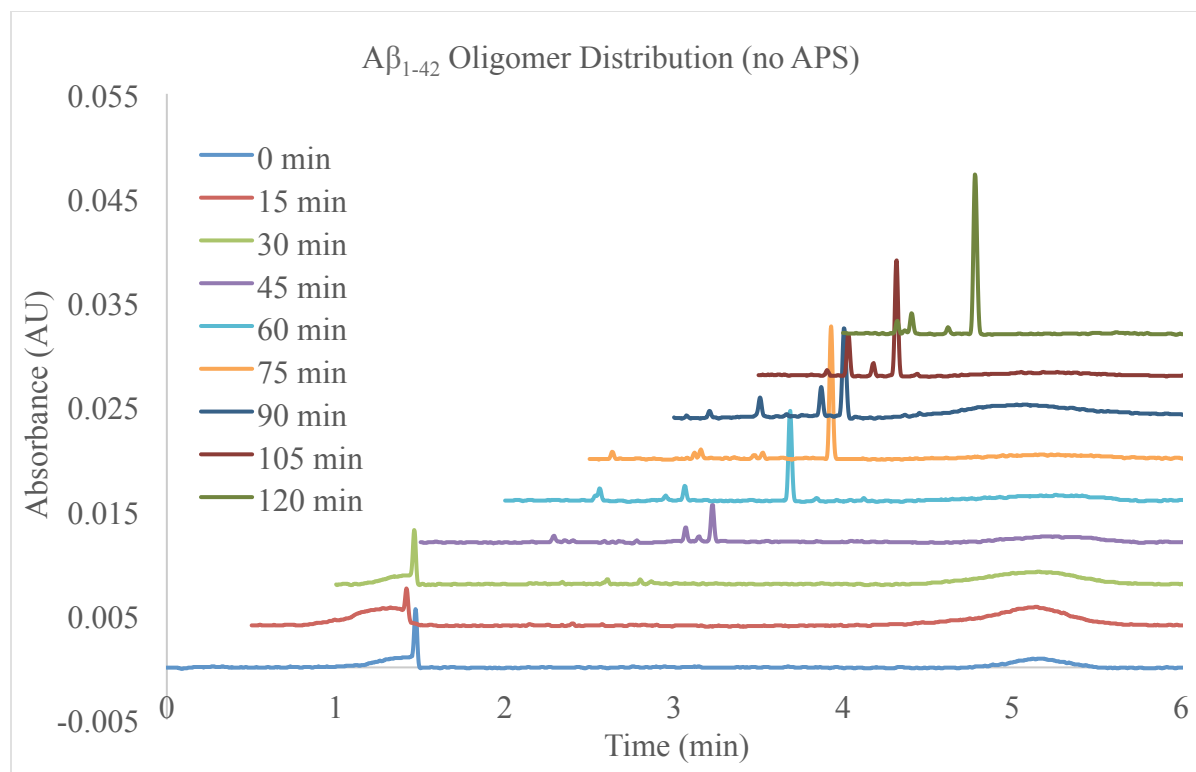


Figure 29: Replication of Figure 19, zoomed in to see a closer view of the initial peaks of the samples.  $A\beta_{1-42}$  was aggregated at 800 rpm for 2 hours. A sample was taken every 15 minutes and subjected to  $Ru(bpy)_3$  and 1 second of Xenon light. The reaction was quenched by placing the sample in the freezer. Each sample was analyzed by CE. Each peak corresponds to protein detection at 214 nm.

It is questionable that Figures 26 and 28 show different peaks of  $A\beta_{1-42}$  after the same aggregation time period. This is likely due to a loss of protein during the dialysis process and inadequate removal of PICUP reactants during dialysis. Presence of APS and  $\beta$ -Mercaptoethanol mask  $A\beta_{1-42}$  and an adequate comparison cannot be made between Figures 26 and 28 due to this. Ultimately, capillary electrophoresis is a more sensitive method to detect  $A\beta_{1-42}$  species when compared to Tris-tricine gels. However, tris-tricine gel analysis takes about 9 hours to analyze 9

samples and CE analysis takes about 13 hours to analyze 9 samples, so this should be taken into account when deciding how to analyze PICUP reactions. Overall, CE analysis shows the amount of  $A\beta_{1-42}$  species increases as aggregation time increases with peaks occurring mainly between 0 and 5 minutes. Tris-tricine analysis shows that  $A\beta_{1-42}$  species decrease between 2 and 37 kDa, but it is likely that higher molecular weight species are forming and cannot be seen.

PICUP and removal of reactants via dialysis was performed three-peat. Unfortunately, the results were limited by the efficiency of dialysis; many of the samples still had residual reactants. This coupled with the loss of protein compromised the visibility of  $A\beta_{1-42}$  peaks. The Hestekin lab was unable to distinctly correlate bands on a Tris-tricine gel to peaks via CE analysis due to this inefficiency. However, when dialysis efficiency was high, CE was a valid method to analyze PICUP samples. Additional experiments should be performed to make dialysis a more consistent method of removing PICUP reactants to greatly affect CE analysis of  $A\beta_{1-42}$  aggregates. Also, more experiments should be performed to confirm the reason for the difference in CE analysis for samples after dialysis and samples not including APS and  $\beta$ -Mercaptoethanol. It would be preferable to perform dialysis rather than eliminate APS as a reactant because its inclusion ensures the most efficient capture of  $A\beta_{1-42}$  oligomers. Ultimately, CE is an acceptable method for analysis of PICUP samples that is more sensitive than Tris-tricine gels.

### **Conclusions and Future Directions**

A device available worldwide that could enhance  $A\beta_{1-42}$  studies would benefit the Alzheimer's research community. A device that can detect  $A\beta_{1-42}$  at a picomolar level and separate metastable species would allow for study of its aggregation pathway and provide a breadth of knowledge about AD. Optimizing the recovery of  $A\beta_{1-42}$  recovery in capillaries by

coating them with a hydrophilic polymer would translate to this device. 2000kDa PEO provided the best recovery at 87% compared to an uncoated capillary recovery of 67%. Further investigation needs to be done for reproducibility.

Studying  $A\beta_{1-42}$  after PICUP application with CE could provide insight to its aggregation pathway because CE has the ability to provide high resolution analysis of photo-crosslinked aggregated  $A\beta_{1-42}$ . These results could provide a toolset to help researchers develop a new way to study this protein since it's metastable nature causes difficulty in obtaining reproducible results. From the experiments conducted by the Hestekin lab, other researchers can use CE and obtain the specific molecular weight of  $A\beta_{1-42}$  species present along the aggregation pathway. Further, if the toxicity of these species was dependent upon the molecular weight a drug could be designed to block or eliminate these species, in order to slow, prevent, or cure Alzheimer's disease.

## References

1. 2014 Alzheimer's Disease Facts & Figures. *Alzheimer's & Dementia*: 2014.
2. Selkoe D. Molecular pathology of the aging human brain. *Trends in Neurosciences*. 1982;5:332-6.
3. Soto C. Protein misfolding and disease: protein refolding and therapy. *FEBS Letters*. 2001;498:204-7.
4. Sisodia S, Price D. Role of the B-amyloid protein in alzheimer's disease. *The FASEB Journal*. 1995;9:366-70.
5. Estrada LD, Soto C. Disrupting B-amyloid aggregation for alzheimer disease treatment. *Current Topics in Medicinal Chemistry*. 2007;7:115-26.
6. Benilova I, Karran E, De Strooper B. The toxic AB oligomer and alzheimer's disease: an emperor in need of clothes. *Nature Neuroscience*. 2012;15(3):349-57.
7. Hardy J, Selkoe D. The amyloid hypothesis of alzheimer's disease: progress and problems on the road to therapeutics. *Science*. 2002;297:353-6.
8. Walsh D, Selkoe D. AB oligomers-a decade of discovery. *Journal of Neurochemistry*. 2007;101:1172-84.
9. Klein W, Krafft G, Finch C. Targeting small AB oligomers: the solution to an alzheimer's disease conundrum? *Trends in Neurosciences*. 2001;24(4):219-24.
10. Necula M, Kaye R, Milton S, Glabe C. Small molecule inhibitors of aggregation indicate that amyloid B oligomerization and fibrillization pathways are independent and distinct. *Journal of Biological Chemistry*. 2007;282(14):10311-24.
11. Bitan G, Fradinger E, Spring S, Teplow D. Neurotoxic protein oligomers- what you see is not always what you get. *Amyloid*. 2005;12(2):88-95.
12. Hefti F, Goure W, Jerecic J, Iverson K, Walicke P, Krafft G. The case for soluble AB oligomers as a drug target in Alzheimer's disease. *Trends in Pharmacological Sciences*. 2013;34(5):261-6.
13. Campioni S, Mannini B, Zampagni M, Pensalfini A, Parrini C, Evangelisti E, et al. A causative link between the structure of aberrant protein oligomers and their toxicity. *Nature Chemical Biology*. 2010;6:140-7.
14. McLean C, Cherny R, Fraser F, Fuller S, Smith M, Beyreuther K, et al. Soluble pool of AB amyloid as a determinant of severity of neurodegeneration in alzheimer's disease. *Annals of Neurology*. 1999;46(6):860-6

15. Kasai T, Tokuda T, Taylor M, Kondo M, Mann D, Foulds P, et al. Correlation of the AB oligomer levels in matched cerebrospinal fluid and serum samples. *Neuroscience Letters*. 2013;551:17-22.
16. Perrin R, Fagan A, Holtzman D. Multimodal techniques for diagnosis and prognosis of alzheimer's disease. *Nature*. 2009;461:916-22.
17. Pryor E, Moss M, Hestekin C. Unraveling the early events of Amyloid-B protein (AB) aggregation: Techniques for the determination of AB aggregate size. *International Journal of Molecular Science*. 2012;13:3038-72.
18. Albarghouthi M, Buchholz B, Huiberts P, Stein T, Barron A. Poly-N0hydroxyethylacrylamide (polyDuramide): a novel, hydrophilic, self-coating polymer matrix for DNA sequencing by capillary electrophoresis. *Electrophoresis*. 2002;23:1429-40.
19. Gilges M, Kleemis M, Schomburg G. Capillary zone electrophoresis: separations of basic and acidic proteins using poly(vinyl alcohol) coatings in fused silica capillaries. *Analytical Chemistry*. 1994;66:2038-46.
20. Bitan G, Teplow D. Rapid photochemical cross linking- a new tool for studies of metastable, amyloidogenic protein assemblies. *Accounts of Chemical Research*. 2004;37(6):357-64.
21. Landers J. *Handbook of capillary and microchip electrophoresis and associated micro techniques*. 3 ed. Boca Raton: CRC Press; 2008.
22. Albarghouthi M, Stein T, Barron A. Poly-n-hydroxyethylacrylamide as a novel, adsorbed coating for protein separation by capillary electrophoresis. *Electrophoresis*. 2003;24:1166-75.
23. Steiner F, Hassel M. Control of electroosmotic flow in non aqueous capillary electrophoresis by polymer capillary coatings. *Electrophoresis*. 2003;24:399-407.
24. Yeung K, Lucy C. Suppression of electroosmotic flow and prevention of wall adsorption in capillary zone electrophoresis using zwitterionic surfactants. *Analytical Chemistry*. 1997;69:3435-41.
25. *Capillary Electrophoresis 2015* [cited 2015]. Available from: [https://en.wikipedia.org/wiki/Capillary\\_electrophoresis](https://en.wikipedia.org/wiki/Capillary_electrophoresis).
26. Bohoyo D, Le Potier I, Rivere C, Klafki H, Wiltfang J, Taverna M. Quantitative CE method to analyse tau protein isoforms using coated fused silica capillaries. *Journal of Separation Science*. 2010;33:1090-8.



27. Doherty E, Meagher R, Albarghouthi M, Barron A. Microchannel wall coatings for protein separations by capillary and chip electrophoresis. *Electrophoresis*. 2003;24:34-54.
28. Belder D, Deege A, Husmann H, Kohler F, Ludwig M. Cross-linked poly(vinyl alcohol) as a permanent hydrophilic column coating for capillary electrophoresis. *Electrophoresis*. 2001;22:3813-8.
29. Buchholz B, Zahn J, Kenward M, Slater G, Barron A. Flow-induced chain scission as a physical route to narrowly distributed, high molar mass polymers. *Polymer*. 2004;45.
30. Fancy D, Kodadek T. Chemistry for the analysis of protein-protein interactions: rapid and efficient cross-linking triggered by long wavelength light. *Proceedings of the National Academy of Scientists*. 1999;96:6020-4.
31. Kotzyba-Hibert F, Kapfer I, Goeldner M. Recent trends in photoaffinity labeling. *Angewandte Chemie International Edition English*. 1995;34:1296-312.
32. Bitan G, Vollers S, Teplow D. Elucidation of primary structure elements controlling early amyloid B-protein oligomerization. *The Journal of Biological Chemistry*. 2003;278(37):34882-9.
33. Bitan G, Lomakin A, Teplow D. Amyloid B-protein oligomerization. *The Journal of Biological Chemistry*. 2001;276(37):35176-84.
34. Bitan G, Kirkitadze M, Lomakin A, Vollers S, Benedek G, Teplow D. Amyloid B-protein assembly: AB40 and AB42 oligomerize through distinct pathways. *Proceedings of the National Academy of Sciences of the United States of America*. 2003;100(1):330-5.
35. Vollers S, Teplow D, Bitan G. Determination of Peptide Oligomerization State Using Rapid Photochemical Crosslinking. *Methods in Molecular Biology*. 2005;299:11-8.

## Appendix

### Monomerization by HFIP and storage of A $\beta$ <sub>1-42</sub> Stock Solutions:

1. A $\beta$ <sub>1-42</sub> is stored as a solid at -80C. Remove and place on ice when ready to prepare stock peptide films.
2. Place 1,1,1,3,3,3-hexafluoro-2-propanol (HFIP) on ice in the hood and allow to cool. HFIP is highly corrosive and very volatile. Add enough HFIP to A $\beta$ <sub>1-42</sub> such that the final peptide concentration is 1mM (e.g. 221.53 ul cold HFIP to 1 mg A $\beta$ <sub>1-42</sub>). Rinse vial thoroughly.
3. Incubate at room temperature for 60 min, keeping vial closed. Solution should be clear and colorless. Any traces of yellow color or cloudy suspension indicate poor peptide quality and should not be used.
4. Separate the HFIP into vials with 0.0271 mg/vial. That means each vial has 6  $\mu$ L stock.
5. Aliquot solution into non-siliconized microcentrifuge tubes. Do not close tubes.
6. Allow HFIP to evaporate overnight in the hood at room temperature.
7. All traces of HFIP must be removed. The resulting peptide should be a thin clear film at the bottom of the tubes. The peptide should not be white or chunky.
8. Store dried peptide films over desiccant at -80C. These stocks should be stable for several months.

### Phosphate Buffer Preparation .1M, pH=7.4

1. Add 19mL of .2M monobasic sodium phosphate
2. Add 81mL of .2M dibasic sodium phosphate
3. Dilute to a total 200mL.

### Sample Preparation

1. Retrieve vial with .0271mg of A $\beta$ <sub>1-42</sub> from the -80°C freezer.
2. Prepare 20 $\mu$ M concentration by adding 15 $\mu$ L of 5mM NaOH.
3. Let dissolve for 5 minutes.
4. Add 285 $\mu$ L of 10mM phosphate buffer.
5. Let dissolve for 15 minutes.
6. If aggregating, place on shaker at 800rpm and 25°C.

### CE Protocol

1. Cut capillary to 31cm using device.
2. Coat capillary using following sequence:
  1. Rinse for 20 minutes with .1M NaOH at 50psi.
  2. Rinse for 20 minutes with water at 20psi.
  3. Rinse for 60 minutes with .1M HCl at 20psi.
  4. Rinse for 10 minutes with water at 20psi.
  5. Rinse for 15 minutes with water at 20psi.
  6. Rinse for 15 minutes with .1M HCl at 20psi.
  7. Rinse for 30 minutes with coating polymer at 50psi.

8. Rinse for 15 minutes with water at 20psi.
9. Rinse for 10 minutes with .1M phosphate buffer at 20psi.
10. Rinse for 10 minutes with water at 50psi.
11. Rinse for 10 minutes with .1M phosphate buffer at 50psi.
3. For coating study reverse runs:
  1. Rinse for 5 minutes with .1M phosphate buffer at 50psi.
  2. Inject sample for 8 seconds at 0.5psi.
  3. Separate for 30 minutes at 7kV with a .17 minute ramp.
4. For coating study forward runs:
  1. Rinse for 5 minutes with .1M phosphate buffer at 50psi.
  2. Inject sample for 8 seconds at 0.5psi.
  3. Separate for 60 minutes at 7kV with a .17 minute ramp.
5. For PICUP samples:
  1. Rinse for 5 minutes with .1M phosphate buffer at 50psi.
  2. Inject sample for 15 seconds at 10.0kV.
  3. Separate for 30 minutes at 7kV with a .17 minute ramp.
6. All sample runs separated by the following wash:
  1. Rinse for 10 minutes with water at 50psi.
  2. Rinse for 10 minutes with .1M phosphate buffer at 50psi.

#### PICUP Protocol

1. Align camera, phototube and light source. Set camera to setting 1.
2. Add 4 $\mu$ L of 20 $\mu$ M A $\beta$ <sub>1-42</sub> to a non-stick microcentrifuge tube.
3. Add 4 $\mu$ L of 10mM Ru(bpy)<sub>3</sub>.
4. Add 4 $\mu$ L of 200mM APS.
5. Insert tube in front of camera.
6. Press shutter to expose sample to light.
7. Quickly add 10 $\mu$ L of 5%  $\beta$ -mercaptoethanol.

#### 16.5%Tris-Tricine Gel Protocol

1. Set up glass plates in Bio-Rad device.
2. Add 80mL of 30% acrylamide, 2.75mL 1.25M TrisCl pH=8.8, .95mL diH<sub>2</sub>O, and 50 $\mu$ L 10% SDS.
3. Quickly add 150 $\mu$ L of 10% APS and 12 $\mu$ L TEMED. Pipet between the glass plates.
4. Pipet a layer of butanol on top of solution.
5. When the gel is polymerized, remove the butanol and replace with spacer.
6. Add 415 $\mu$ L of 30% acrylamide, 630 $\mu$ L of .5M TrisCl pH=6.8, 1.385mL of diH<sub>2</sub>O, and 0.025mL of 10%SDS.
7. Quickly add 75 $\mu$ L of 10% APS and 12 $\mu$ L TEMED. Wait for the gel to polymerize.
8. Place the gel in a 1X Tris-Tricine Running Buffer.
9. Add 7 $\mu$ L of standards and 22 $\mu$ L of sample in the lanes.

#### 12.5% Tris-Glycine Gel Protocol

1. Set up glass plates in Bio-Rad device.

2. Add 2.1mL of 30% acrylamide, .65mL 1.5M TrisCl pH=8.8, 1.55mL diH<sub>2</sub>O, and .7mL of 75% Sucrose.
3. Quickly add 50μL of 10% APS and 3μL TEMED. Pipet between the glass plates.
4. Pipet a layer of butanol on top of solution.
5. When the gel is polymerized, remove the butanol and replace with spacer.
6. Add .375mL of 30% acrylamide, .625mL of .5M TrisCl pH=6.8, and 1.5mL of diH<sub>2</sub>O.
7. Quickly add 22.5μL of 10% APS and 11μL TEMED. Wait for the gel to polymerize.
8. Place the gel in a 1X Tris-Glycine Running Buffer.
9. Add 7μL of standards and 22μL of sample in the lanes.

#### Silver Stain Protocol

1. Let gel soak in fixing solution and shake for 60 minutes. (7.5mL ethanol, 2.5mL glacial acetic acid, water to 25mL).
2. Remove the solution. Let gel soak in sensitizing solution and shake for 1 hour up to 24 hours. (7.5mL ethanol, 1mL sodium thiosulfate, 1.7g sodium acetate, water to 25mL, add 125μL glutaraldehyde before use)
3. Remove the solution. Let gel soak in water three times and shake for 15 minutes each time.
4. Remove the solution. Let gel soak in silver solution and shake for 1 hour. (2.5mL silver nitrate solution, water to 25 mL)
5. Remove the solution. Let gel soak in water twice and shake for 1 minute each time.
6. Remove the solution. Let gel soak in developing solution and shake for 4-6 minutes. (.625g sodium carbonate, water to 25mL, add 20μL of formaldehyde)
7. Remove the solution. Let gel soak in stop solution. (.365g EDTA solution, water to 25mL)
8. Remove gel from solution and scan.

#### Matlab Code

```
%This is a function that takes the output of the 32 Karat program and
%turns the output into time, absorbance, voltage, and current. Then
%located peaks from the data and from each peak the molecular weight.
```

```
d=input('Was Walter run in reverse (1) or forward (2)?');
if d==1
    Ld=10;           %Length to detector, cm
elseif d==2
    Ld=21;
else
    disp('Error d must equal 1 or 2.');
```

```
end
Lt=.31/100;        %Total length of capillary, cm
AB=input('Are you using Amyloid Beta 40 or 42?');
if AB == 40
```

```

    mu_o=13;                %Mobility in free buffer
    Vm=.7362;              %Partial specific Volume, cm3 g-1
elseif AB == 42
    mu_o=13;
    Vm=.7362;
else disp ('Error AB must be of 40 or 42 amino acids.')

end
phi=input('What is the polymer concetration (wt%)?');
if phi > 4
    disp('Concentration must be between 0 and 4 %.');
elseif phi <0
    disp('Concentration must be between 0 and 4 %.');
end

%% Part 1: Analyze data into matrices of Time, AU, kV, uA
%%Ask for file to manipulate into Absorbance and Current data.

[FileName, PathName]=uigetfile('*.xlsx') ;

%Translate data into a numerical array.

[num]=xlsread(FileName);

%Translate numerical array into 4 column matrices of data.

A=num(:,1);
B=num(1:13,2);
C=num(1:13,3);
D=num(1:13,3);

%Create time matrix from imported data.

Rate=B(8);
TotalPts=B(9);
Xmult=B(12);
s=Xmult/Rate;
t=[s:s*s*TotalPts]';

%Separate column A into three separate matrices for Absorbance, Voltage,
%and Current, repectively.

A1=A(14:B(9)+13);
B1=A(B(9)+14:B(9)+C(9)+13);
C1=A(B(9)+C(9)+14:B(9)+C(9)+D(9)+13);

```

```
%Calculate Absorbance, Voltage, and Current.
```

```
AU=A1*B(13);  
kV=B1*C(13);  
uA=C1*D(13);
```

```
%Plot Absorbance and Current versus time on same plot.
```

```
[AX,H1,H2]=plotyy(t,AU,t,uA);  
title (FileName);  
xlabel ('Time(minutes)');  
ylabel (AX(1),'Absorbance (AU)');  
ylabel (AX(2),'Current (\muA)');  
legend('Absorbance','Current');  
set(AX(2),'XTickLabel','','XAxisLocation','Top'); %Make top label.  
set(AX(1),'ylim',[min(AU) max(AU)]); %Set left y limits.  
set(AX(2),'ylim',[min(uA) max(uA)]); %Set right y limits.  
set(AX(1),'xlim',[t(1) t(end)]); %Set left x limits.  
set(AX(2),'xlim',[t(1) t(end)]); %Set right x limits.  
set(AX(1),'box','off') %Turn off left y limits showing on right y.  
set(AX(1),'ytick',linspace(min(AU),max(AU),10)) %Display 10 ticks on left y axis.  
set(AX(2),'ytick',linspace(min(uA),max(uA),5)) %Display 5 ticks on right y axis.
```

```
%% Part 2 Reduce noise, correct baseline, identify peaks
```

```
[p,c,mu]=polyfit(t,AU,40); %Fit electropherogram to a 40th order polynomial  
AU1=polyval(p,t,AU,mu); %Detrend fit from polynomial  
AUcorr=AU-AU1; %Electropherogram with corrected baseline  
WT=ndwt(AUcorr,10,'db8'); %Apply Daubachies8 wavelet transform, Level 10  
AUa=indwt(WT,'a',1); %Reconstruct low pass content  
AUd=indwt(WT,'d',1); %Reconstruct high pass content  
erra=max(abs(AU(:)-AUa(:))); %Calculate the error Wavelet  
noise=max(AUd)-min(AUd); %Calculate the noise taken from the data  
figure(); %Create new plot  
plot(t,AUa);  
title (FileName);  
xlabel ('Time (minutes)');  
ylabel ('Absorbance (AU)');  
xlim ([t(1) t(end)]);  
ylim ([min(AUa) max(AUa)]);
```

```
%Find the peaks that are 30*high of noise value and at least 25 data  
%points apart. Plot the found peaks with markers on the Absorbance graph  
%with noise removed.  
[ph,ploc]=findpeaks(AUa,'minpeakheight',30*noise, 'minpeakdistance',25);
```

```

hold on;
plot(t(ploc),ph,'k^','markerfacecolor',[1 0 0]);
hold off;
tm=t(ploc);           %Create a time matrix of the found peaks

figure()             %Plot the Absorbance before and after noise removal on
same figure
subplot(211)
plot(t,AUcorr)
title ('Absorbance before noise removal')
xlabel ('Time (minutes)');
ylabel ('Absorbance (AU)');
xlim ([t(1) t(end)]);
ylim ([min(AUcorr) max(AUcorr)]);
subplot(212)
plot(t,AUa)
title ('Absorbance after noise removal')
xlabel ('Time (minutes)');
ylabel ('Absorbance (AU)');
xlim ([t(1) t(end)]);
ylim ([min(AUa) max(AUa)]);

%% Part 3 Calculate molecular weight.

V=mean(kV);         %Calculate applied voltage (kV)

%Create Ferguson plot

muf=[13 9 8 7 6];   %Ferguson plot, mobility
mu_of=13;           %Ferguson plot, free mobility
phif=[0 1 2 3 4];   %Ferguson plot, polymer concentration
figure();           %Create Ferguson Plot
plot(phif,log10(muf/mu_of));
title 'Ferguson Plot Amyloid Beta 1-42';
xlabel 'Polymer Concentration (%)';
ylabel 'Mobility log(\mu^\muo)';
for i=1:length(tm); %Calculate the mobility of each peak
mu(i)=((Ld*Lt)/V)*(1/tm(i));
i=i+1;
end;
for j=1:length(mu); %Create a matrix of phi for each peak
phim(j)=phi;
j=j+1;
end;

```

```

hold on;
plot(phim,mu,'k^','markerfacecolor',[1 0 0]); %Plot each peak on Ferguson plot
KR=(-log10(mu/mu_o))/phi; %Protein retardation coefficient
l=1000*10^-7; %Total length of polymer fiber/volume, cm^-2
r=250*10^-7; %Polymer fiber radius, cm
R=sqrt(KR/(pi*1*10^-16))-r; %Protein radius, cm
N=6.0221413*10^23; %Avogadros number
Mw=(R/10^7).^3*((4*pi*N)/(3*Vm)); %Molecular weight, Da
VN={'MigrationTime' 'Mobility' 'Radius' 'MW'};
Data=table(tm,mu,R,Mw,'VariableNames',VN);

```